

Semiclassical gravity phenomenology under the causal-conditional quantum measurement prescription II: Heisenberg picture and apparent optical entanglement

Yubao Liu,¹ Wenjie Zhong,¹ Yanbei Chen,^{2,*} and Yiqiu Ma^{1,3,†}

¹*Center for Gravitational Experiment, Hubei Key Laboratory of Gravitation and Quantum Physics, School of Physics, Huazhong University of Science and Technology, Wuhan, 430074, China*

²*Burke Institute of Theoretical Physics, California Institute of Technology, Pasadena, CA, 91125, USA*

³*Department of Astronomy, School of Physics, Huazhong University of Science and Technology, Wuhan, 430074, China*

The evolution of quantum states influenced by semiclassical gravity is distinct from that in quantum gravity theory due to the presence of a state-dependent gravitational potential. This state-dependent potential introduces nonlinearity into the state evolution, of which the theory is named Schrödinger-Newton (SN) theory. The formalism for understanding the continuous quantum measurement process on the quantum state in the context of semiclassical gravity theory has been previously discussed using the Schrödinger picture in Paper I[1]. In this work, an equivalent formalism using the Heisenberg picture is developed and applied to the analysis of two optomechanical experiment protocols that targeted testing the quantum nature of gravity. This Heisenberg picture formalism of the SN theory has the advantage of helping the investigation of the covariance matrices of the outgoing light fields in these protocols and further the entanglement features. We found that the classical gravity between the quantum trajectories of two mirrors under continuous quantum measurement in the SN theory can induce an apparent entanglement of the outgoing light field (though there is no quantum entanglement of the mirrors), which could serve as a false alarm for those experiments designed for probing the quantum gravity induced entanglement.

I. INTRODUCTION

In the quantum era, advancements in modern quantum technology have paved the way for experimental investigations into the characteristics of gravitational fields generated by quantum objects [2–13]. The initial step in these explorations involves conducting experiments that can assess the quantum aspects of gravitational fields [14–17]. Generally, a gravitational field comprises a near-zone Newtonian component (Newtonian gravity) and transverse wave components (gravitational waves). Several studies present compelling arguments suggesting that demonstrating the quantum nature of Newtonian gravity strongly indicates the quantum nature of gravitational waves [18–20]. Consequently, these arguments encourage us to concentrate on testing the quantum characteristics of Newtonian gravity, which is substantially more feasible than directly probing the quantum nature of gravitational waves.

The fundamental design principle of these experiments is to identify observational signatures that can differentiate between quantum gravity and semi-classical gravity theories [19, 21–25]. These two theoretical frameworks are distinguished by their treatment of the gravitational field: quantum gravity posits that the gravitational field represents a quantum degree of freedom (d.o.f.) capable of existing in superposition states and transmitting quantum information [18–20, 26–29]. Accordingly, the joint quantum state of gravitational and matter degrees of freedom evolves *linearly* within their *joint Hilbert space*. In contrast, the semi-classical gravity theory maintains the classical spacetime curvature $G_{\mu\nu}$, which is sourced by the quantum expectation value of the matter's energy-momentum tensor, $\langle \psi | \hat{T}_{\mu\nu} | \psi \rangle$, where $|\psi\rangle$ represents the quantum state of the matter [30, 31]. In other words, in the context of semi-classical gravity, the gravitational potential is dependent on the state of the system. Notably, in the non-relativistic limit, such a *state-dependent gravitational potential* influences the evolution of $|\psi\rangle$, resulting in a *nonlin-*

ear evolution as described by the *Schrödinger-Newton (SN) equation* [32–37]. Consequently, by examining the gravity-induced quantum state evolution, one can extract observational signatures that distinguish between quantum and classical gravity interactions [38–45][46].

An intriguing and promising type of experiment involves exploring the quantum nature of gravity by examining quantum correlations and entanglements generated by *quantum Newtonian gravity*, as proposed in [18–20, 47, 48]. Experimental protocols for testing these gravity-induced entanglements (GIE) include gravitationally coupled spin systems [18] and mechanical oscillator systems [19]. In the latter case, the GIE is probed via an optical field that couples with the mechanical oscillators. Essentially, the GIE of the two mechanical oscillators is mapped onto two optical fields, creating correlations and entanglement between the optical fields. On the contrary, in the Schrödinger-Newton (SN) scenario where mutual gravity is classical, the two mechanical oscillators cannot establish entanglement through a classical channel. Thus, previous work [19] concludes that there will be no correlations or entanglement in the optical fields in the SN theory. Therefore, the presence of correlation or entanglement in the outgoing light fields serves as a definitive indicator of quantum gravity.

However, this result, while insightful, requires careful examination, as we demonstrated in our previous work [1], referred to as Paper I herein. Paper I introduced a "causal-conditional formalism" to address the process of continuous quantum measurement of a mechanical quantum state in the SN theory. The findings reveal that classical gravity generated by the quantum trajectories [3, 49] of two oscillator mirrors can also induce a *correlation* in the outgoing light field, which is nearly indistinguishable from that induced by quantum gravity. These quantum trajectories result from the continuous quantum measurement of both mirrors.

The correlation of light identified in Paper I does not imply a quantum correlation between the mirrors, as classical

gravity cannot transmit quantum information [50–52]. Consequently, this work demonstrates that examining the statistical properties of light might mistakenly suggest the presence of a quantum correlation between mirrors, potentially resulting in a false indication of quantum gravity. However, in the context of GIE-experiments, our primary interest lies in determining whether the SN theory could similarly create a misleading signal when the light field's entanglement, which represents a specific form of correlation, is assessed. Within the SN framework, analyzing the entanglement structure of outgoing optical fields necessitates new theoretical approaches.

As discussed in Section III, the conditional density matrix approach we developed in Paper I, based on the Schrödinger picture, has limitations. It cannot compute the covariance matrix of the outgoing light and is thus unsuitable for investigating the entanglement structure. Consequently, Paper I does not determine whether this light correlation, induced by the classical-gravity-coupled quantum trajectories, implies a false alarm of GIE. In standard quantum mechanics, the logarithmic negativity [53–55] quantitatively measures the entanglement of a joint quantum Gaussian state, determined by the covariance matrix of the outgoing light. To address the question of correlation nature, we require an alternative approach in the *Heisenberg picture* to handle the continuous quantum measurement of oscillator mirrors in the SN theory and calculate this covariance matrix. Methodologically, this work will develop such an approach, demonstrating its equivalency to the conditional density matrix method.

Addressing this question is crucial for testing the quantum nature of gravity. Calculations in this paper will show that the quantum correlation of outgoing lights induced by classical gravity indeed constitutes an entanglement-like structure (named apparent entanglement), closely resembling the optical entanglement induced by quantum gravity. (false alarm, mirror no entanglement). Careful interpretation of GIE experimental results involving quantum measurement is essential.

The structure of this paper is organized as follows. In Section II, a review of the main results obtained in Paper I is presented, including an introduction to the setup of the experimental protocol. Section V is devoted to the development of the method based on the Heisenberg picture, which allows us to compute the covariance matrix of the outgoing light. The equivalency of this Heisenberg-picture method to the conditional master equation method will be explicitly presented. Section VII will apply the method developed in Section V to the optomechanical protocol for detecting gravity-induced entanglement. The physical interpretation of the result will be thoroughly discussed in Section VII and finally we will conclude the paper.

II. OPTOMECHANICAL SYSTEM AFFECTED BY SEMI-CLASSICAL GRAVITY

Before introducing the Heisenberg-picture method in SN theory, we will outline the optomechanical protocols designed to test the quantum nature of gravity .

In Paper I, two optomechanical protocols are discussed, termed the "self-gravity protocol" and "mutual gravity protocol" (see Fig. 2). Although the optical entanglement issue in this paper arises from the mutual gravity protocol, the first protocol is essential for developing and illustrating the Heisenberg-picture method.

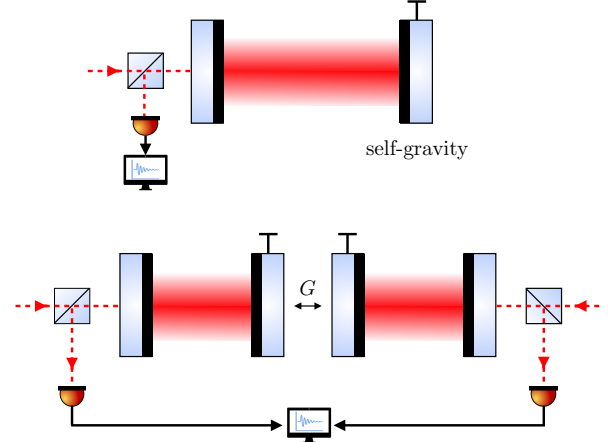


FIG. 1. Optomechanical protocol for testing SN theory. Upper panel: self-gravity protocol, lower panel: mutual gravity protocol.

The self-gravity protocol is an optomechanical system affected by the mirror's self-gravity field. When gravity is classical, this self-gravity potential depends on the quantum state of the mirror's center-of-mass (CoM) motion [21]. Information about the mirror's CoM motion is transferred into the light field through optomechanical coupling. The SN Hamiltonian is given by:

$$\hat{H}_{\text{self,SN}} = \frac{\hat{p}^2}{2M} + \frac{1}{2}M\omega_m^2\hat{x}^2 + \frac{1}{2}M\omega_{\text{SN}}^2(\hat{x} - \langle \hat{x} \rangle)^2 + \hbar\alpha\hat{a}_1\hat{x}, \quad (1)$$

where α represents the optomechanical measurement strength and \hat{a}_1 is the amplitude quadrature operator of the light field. The SN term describes the state-dependent self-gravity effect, with the SN frequency [21] $\omega_{\text{SN}} = \sqrt{Gm/6\sqrt{\pi}x_{\text{zp}}^3}$, with the m, x_{zp} are the ion mass and zero-point displacement of the ion oscillates in the crystal field, respectively. The first two terms describe the Hamiltonian of a free mechanical oscillator without gravity effects. When gravity is quantum, the self-gravity effect is negligible, rendering the SN term absent [21]:

$$\hat{H}_{\text{self,QG}} = \frac{\hat{p}^2}{2M} + \frac{1}{2}M\omega_m^2\hat{x}^2 + \hbar\alpha\hat{a}_1\hat{x} + o(G^2), \quad (2)$$

The mutual gravity protocol was introduced in [19], where two mechanical oscillators (A,B) are coupled via their mutual gravity. In the classical gravity scenario, the corresponding Hamiltonian (mechanical part) is:

$$\hat{H}_{m,\text{SN}} = \sum_{A/B} \left[\frac{\hat{p}_{A/B}^2}{2M} + \frac{M\omega_m^2}{2}\hat{x}_{A/B}^2 - \mathcal{C}(\hat{x}_{A/B} - \langle \hat{x}_{B/A} \rangle)^2 \right], \quad (3)$$

where $\mathcal{C} = M\Lambda G\rho$, with Λ, ρ being the geometric factor and mass density of the oscillator mirrors, respectively. Under quantum gravity, the Hamiltonian is modified to:

$$\hat{H}_{m,\text{QG}} = \sum_{A/B} \left[\frac{\hat{p}_{A/B}^2}{2M} + \frac{M\omega_m^2}{2} \hat{x}_{A/B}^2 - \mathcal{C}(\hat{x}_{A/B} - \hat{x}_{B/A})^2 \right]. \quad (4)$$

Two light fields independently couple to the mechanical oscillators as follows:

$$\hat{H}_{\text{int}} = -\hbar\alpha(\hat{a}_1\hat{x}_A + \hat{b}_1\hat{x}_B), \quad (5)$$

assuming both light fields have the same coherent amplitude α .

In these two protocols, the motion of the test mass mirrors is probed through their continuous coupling with the optical field. When the phase quadrature of the outgoing field is measured, it collapses the opto-mechanical joint quantum state. This collapse leaves the mirror's quantum trajectory, which can have a significant impact on the SN dynamics.

III. CAUSAL CONDITIONAL DYNAMICS IN THE SCHRÖDINGER PICTURE

This section provides an overview of the conditional master equation method as discussed in Paper I, elucidating why this approach is inadequate for analyzing gravity-induced optical entanglement. Additionally, the result in Paper I is re-derived from the filtering problem perspective. This re-derivation will be instrumental in demonstrating the equivalence between the Heisenberg-picture method and the conditional master equation method.

A. Causal conditional approach to continuous quantum measurement

Consider the optomechanical system as an example of a continuous quantum measurement process [3, 56–58]. During each infinitesimal temporal interval, entanglement is established between the incoming light fields and the mechanical oscillator, followed by a projective measurement of the outgoing light fields. This projective optical measurement collapses the joint quantum state into the Hilbert space of the mechanical oscillator, thereby generating a conditional mechanical state. This process occurs continuously, with the mean position and momentum of the conditional mechanical state tracing a *quantum trajectory* in phase space [3, 49]. This is referred to as the *causal conditional formalism*, which characterizes continuous quantum measurement processes. It is important to note that this causal conditional formalism is entirely equivalent to the pre-selection and post-selection formalism in standard quantum mechanics [59].

However, as discussed in [22] and Paper I, this equivalency breaks down under the SN theory. The primary reason lies in the quantum evolution (or Hamiltonian) of the mechanical

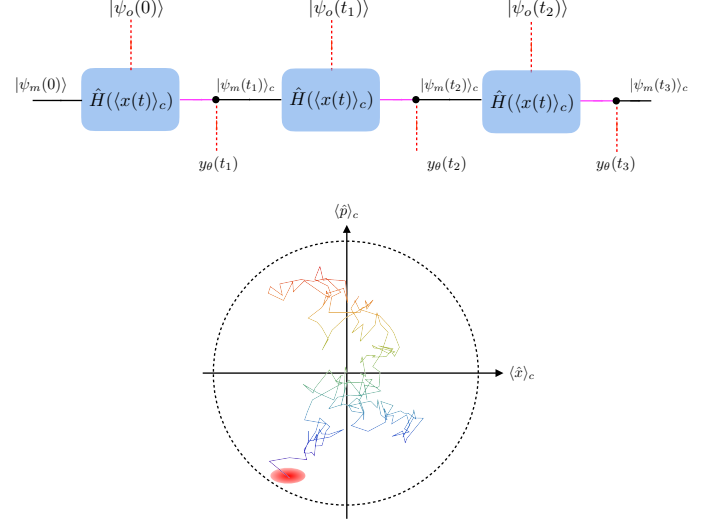


FIG. 2. Causal conditional evolution in the Schrödinger picture. The optomechanical entangled state, created by ponderomotive interaction, evolves under the SN nonlinear Hamiltonian. This state is projected into the mechanical Hilbert space and creates a conditional mechanical state that sources the self-gravity. The red, black, and magenta line describes the optical, mechanical, and optomechanical joint states, respectively. The lower panel illustrates the quantum trajectory, and the SN term will also fluctuate with the random evolution of the conditional mean mechanical displacement $\langle x \rangle_c$.

oscillator, which depends non-linearly on the quantum state. Specifically, within the *pre/post-selection formalism*, the $\langle \hat{x} \rangle$ in Eqs. (1) and (3) represents the expectation value of \hat{x} concerning the *initial/final mechanical state*. In contrast, under the *causal conditional formalism*, $\langle \hat{x} \rangle$ denotes the expectation value of \hat{x} concerning the *conditional mechanical state*. Consequently, the quantum trajectory generates classical gravity as the conditional mean of the mechanical displacement follows the quantum trajectory. Paper I investigated the causal conditional formalism within the Schrödinger picture and established a stochastic master equation to describe the evolution of the mechanical state under SN theory, as briefly summarized below.

B. Stochastic master equation and quantum trajectory

For illustration, we first consider the self-gravity protocol. The stochastic master equation derived in Paper I is:

$$d\hat{\rho} = -\frac{i}{\hbar}[\hat{H}_0, \hat{\rho}]dt + \frac{\alpha}{\sqrt{2}} \sin \theta \{\hat{x} - \langle \hat{x} \rangle_c, \hat{\rho}\}dW - \frac{i\alpha}{\sqrt{2}} \cos \theta [\hat{x}, \hat{\rho}]dW - \frac{\alpha^2}{4} [\hat{x}, [\hat{x}, \hat{\rho}]]dt, \quad (6)$$

where $\hat{\rho}$ is the mirror's conditional density matrix, and \hat{H}_0 is the Hamiltonian from Eq. (1) with $\alpha = 0$. The projective measurement on the outgoing light contributes the Lindblad and Ito terms. In this equation, the θ -quadrature of the outgoing

field $\hat{a}_\theta = \hat{a}_1 \cos \theta + \hat{a}_2 \sin \theta$ is measured, where \hat{a}_1 and \hat{a}_2 are amplitude and phase quadratures, respectively.

The quantum trajectory can be derived from this master equation:

$$\begin{aligned} d\langle \hat{x} \rangle_c &= \frac{\langle \hat{p} \rangle_c}{M} dt + \sqrt{2}\alpha \sin \theta V_{xx} dW, \\ d\langle \hat{p} \rangle_c &= -M\omega_m^2 \langle x \rangle_c dt - \gamma_m \langle \hat{p} \rangle_c dt + \sqrt{2}\alpha \sin \theta V_{xp} dW \quad (7) \\ &\quad + \frac{\hbar\alpha}{\sqrt{2}} \cos \theta dW, \end{aligned}$$

where V_{xx} and V_{xp} are second-order conditional moments satisfying Riccati equations:

$$\begin{aligned} \dot{V}_{xx} &= \frac{2V_{xp}}{M} - 2\alpha^2 \sin^2 \theta V_{xx}^2, \\ \dot{V}_{xp} &= -\gamma_m V_{xp} + \frac{V_{pp}}{M} - M\omega_q^2 V_{xx} - 2\alpha^2 \sin^2 \theta V_{xx} V_{xp} \\ &\quad - \hbar\alpha^2 \sin \theta \cos \theta V_{xx}, \quad (8) \\ \dot{V}_{pp} &= -2\gamma_m V_{pp} - 2M\omega_q^2 V_{xp} - 2\alpha^2 \sin^2 \theta V_{xp}^2 + \frac{\hbar^2 \alpha^2}{2} \\ &\quad - 2\hbar\alpha^2 \sin \theta \cos \theta V_{xp} - \frac{\hbar^2 \alpha^2}{2} \cos^2 \theta. \end{aligned}$$

The measurement record of the output light is:

$$\tilde{y}_\theta = \alpha \sin \theta \langle \hat{x} \rangle + \frac{dW}{\sqrt{2}dt}. \quad (9)$$

To determine the statistical properties of the data series $y_\theta(t)$, integrate Eq. (7) to find the conditional mean $\langle \hat{x}(t) \rangle_c$ at the long-time tail:

$$\begin{aligned} \langle \hat{x}(t) \rangle_c &= \sqrt{2}\alpha \int_0^t dW(s) e^{-\frac{\gamma_m}{2}(t-s)} \left(\frac{\hbar}{2M\tilde{\omega}_m} \sin \tilde{\omega}_m(t-s) \cos \theta \right. \\ &\quad + V_{xx}(s) \left[\cos \tilde{\omega}_m(t-s) + \frac{\gamma_m}{2\tilde{\omega}_m} \sin \tilde{\omega}_m(t-s) \right] \sin \theta \\ &\quad \left. + V_{xx}^2(s) \frac{\alpha^2}{\tilde{\omega}_m} \sin^3 \theta \right), \quad (10) \end{aligned}$$

where the initial condition is ignored, and $\tilde{\omega}_m \equiv$

$\sqrt{\omega_m^2 - \gamma_m^2}/4$. With $\theta = \pi/2$ and using the approximation $\tilde{\omega}_m \approx \omega_m$, this formula reduces to the approximated case Eq.(11) in Paper I.

Using the Ito formula:

$$\begin{aligned} \langle dW(t)dW(t') \rangle &= \frac{1}{T} \int_0^T dW(t+\tilde{t})dW(t'+\tilde{t})d\tilde{t} \quad (11) \\ &= dt dt' \delta(t-t'), \end{aligned}$$

and the measurement record formula Eq.(9), derive:

$$S_{y_\theta y_\theta}(\Omega) = \frac{|A_q^\theta(\Omega) - R_m(\Omega)|^2}{|R_m(\Omega)|^2}, \quad (12)$$

where

$$\begin{aligned} A_q^\theta(\Omega) &= V_{xx} \alpha^2 [V_{xx} \alpha^2 \cos 2\theta - V_{xx} \alpha^2 - 2(\gamma_m - i\Omega)] \sin^2 \theta \\ &\quad - \alpha^2 \sin \theta \cos \theta / M, \\ R_m(\Omega) &= \omega_m^2 - \Omega^2 - i\gamma_m \Omega. \end{aligned} \quad (13)$$

Assuming $\theta = \pi/2$, the spectrum simplifies to:

$$S_{\tilde{y}_{\pi/2} \tilde{y}_{\pi/2}} = \frac{4V_{xx} \alpha^2 (V_{xx} \alpha^2 + \gamma_m) (V_{xx} \alpha^2 ((V_{xx} \alpha^2 + \gamma_m) + \omega_m^2))}{M^2 |\omega_m^2 - \Omega^2 - i\gamma_m \Omega|^2}, \quad (14)$$

where V_{xx} is the steady-state value determined by the Riccati equation, as given in Eq. (8). In the high- Q limit, this result is consistent with those presented in Paper I.

C. Revisit the solution of the master equation as a filtering problem

The foregoing result can be re-derived from an alternative perspective, which will be valuable for comparison with the Heisenberg-picture approach discussed in the next section. Essentially, the quantum trajectory equations Eqs.(7) have already contained the relationship between the measurement records and the conditional mean $(\langle x(t) \rangle_c, \langle p(t) \rangle_c)$. This relationship can be easily seen by representing the Ito term in quantum trajectory equations in terms of the measurement record (see Eq. (9)):

$$\frac{d}{dt} \begin{bmatrix} \langle \hat{x} \rangle_c \\ \langle \hat{p} \rangle_c \end{bmatrix} = \begin{bmatrix} -2\sin^2 \theta \alpha^2 V_{xx} \\ -M\omega_m^2 - 2\sin^2 \theta \alpha^2 V_{xp} - \hbar\alpha^2 \sin \theta \cos \theta \end{bmatrix} \begin{bmatrix} \langle \hat{x} \rangle_c \\ \langle \hat{p} \rangle_c \end{bmatrix} + \begin{bmatrix} 1/M \\ -\gamma_m \end{bmatrix} \begin{bmatrix} 2\sin \theta \alpha V_{xx} \\ 2\sin \theta \alpha V_{xp} + \hbar\alpha \cos \theta \end{bmatrix} \tilde{y} \quad (15)$$

The solution of the above equation can be written as:

$$\begin{aligned} \langle \hat{x}(t) \rangle_c &= e^{-\Gamma t} \left[x_0 \cos(\Omega_x t) + \frac{p_0}{M\omega_m} \sin(\Omega_x t) \right] \\ &\quad + \int_{t_0}^t dt' K_\theta(t-t') \tilde{y}_\theta(t'). \end{aligned} \quad (16)$$

The filter function $K_\theta(t-t')$ is defined as:

$$\begin{aligned} K_\theta(t-t') &= 2\alpha \sin \theta e^{-\Gamma(t-t')} V_{xx}(t') \cos \Omega_x(t-t') \\ &\quad + 2\alpha e^{-\Gamma(t-t')} \left[\frac{\cos \theta + M V_{xx}(t') \gamma_m \sin \theta}{2M\Omega_x} \sin \Omega_x(t-t') \right], \end{aligned} \quad (17)$$

where

$$\Gamma = \frac{\gamma_m + V_{xx}\alpha^2 \sin^2 \theta}{2}, \quad (18)$$

and

$$\Omega_x^2 = \frac{(3V_{xx}^2\alpha^4 + 4V_{xx}\alpha^2\gamma_m - 2\gamma_m^2 + 8\omega_m^2) + V_{xx}^2\alpha^4 \cos(4\theta)}{8} + \frac{\alpha^2 \sin(2\theta)/M - V_{xx}\alpha^2(V_{xx}\alpha^2 + \gamma_m) \cos(2\theta)}{2}. \quad (19)$$

When we consider the long-term behavior ($t \gg 1/\Gamma$), the initial condition will be forgotten and we have a mapping relation between $\langle \hat{x}(t) \rangle_c$ and $y_\theta(t')$ with the filter function $K_\theta(t - t')$ defined in Eq. (17), which is equivalent to Eq. (10). Moreover, in the above derivation, we used the approximation that the solutions of the Riccati equation will quickly converge to the steady state, i.e. $V_{xx}(t)$ is a constant:

$$V_{xx} = \frac{-\gamma_m}{2\alpha^2 \sin^2 \theta} + \frac{\sqrt{\gamma_m^2 - 2\omega_q^2 - \Lambda^2 \sin 2\theta + 2\sqrt{\omega_q^4 + \Lambda^4 \sin^2 \theta + \Lambda^2 \omega_q^2 \sin 2\theta}}}{2\alpha^2 \sin^2 \theta}. \quad (20)$$

where $\Lambda = \alpha\sqrt{\hbar/M}$.

By applying the Fourier transformation to Eq.,(17), we derive the filter function in the frequency domain:

$$\langle x(\Omega) \rangle_c = K_\theta(\Omega)\tilde{y}_\theta(\Omega) \\ K_\theta(\Omega) = \frac{A_q^\theta(\Omega)}{\alpha \sin \theta(A_q^\theta(\Omega) - R_m(\Omega))}. \quad (21)$$

When combined with the Fourier form of Eq.,(9):

$$\tilde{y}_\theta(\Omega) = \alpha \sin \theta \langle x(\Omega) \rangle_c + dW(\Omega)/\sqrt{2}, \quad (22)$$

one can easily rederive Eq.,(12).

Similar findings for the mutual gravity protocol are discussed in Paper I. However, a notable limitation of the stochastic master equation approach is its inability to investigate the entanglement structure of the outgoing lights within the mutual gravity protocol.

D. Limitations of stochastic master equation

The quantum entanglement of a bipartite Gaussian state can be characterized by the logarithmic negativity ε_N , which is defined as:

$$\varepsilon_N = \max\{-(1/2)\ln \left[\left(\Sigma - \sqrt{\Sigma^2 - 4\det\sigma} \right) / 2 \right], 0\} \quad (23)$$

with $\Sigma = \det\sigma_A + \det\sigma_B - 2\det\sigma_{AB}$,

$$\sigma_A = \begin{bmatrix} S_{\tilde{y}_{1A}\tilde{y}_{1A}} & S_{\tilde{y}_{1A}\tilde{y}_{2A}} \\ S_{\tilde{y}_{2A}\tilde{y}_{1A}} & S_{\tilde{y}_{2A}\tilde{y}_{2A}} \end{bmatrix}, \quad \sigma_{AB} = \begin{bmatrix} S_{\tilde{y}_{1A}\tilde{y}_{1B}} & S_{\tilde{y}_{1A}\tilde{y}_{2B}} \\ S_{\tilde{y}_{2A}\tilde{y}_{1B}} & S_{\tilde{y}_{2A}\tilde{y}_{2B}} \end{bmatrix}, \quad (24)$$

where $\tilde{y}_{1A/B}, \tilde{y}_{2A/B}$ are the recorded data strings when measuring the amplitude and phase quadratures of the outgoing light fields. To obtain the logarithmic negativity ε_N , the covariance matrices σ_A and σ_{AB} are required [53, 54].

However, computing cross-correlation terms such as $S_{\tilde{y}_{1A}\tilde{y}_{2A}}$ via the stochastic master equation approach is not feasible. This limitation arises because the stochastic master equation is derived for a fixed measurement quadrature angle θ , and the ensemble average with respect to the Ito term dW can only be performed for \tilde{y}_θ . Calculating the correlation between \tilde{y}_θ and $\tilde{y}_{\theta'}$ are not meaningful within this framework.

This problem also exists in standard quantum mechanics and quantum gravity cases; however, it can be circumvented using the Heisenberg-picture approach (e.g. the method used in [19]). Therefore, to compute the cross-correlation function in the SN theory, a corresponding Heisenberg picture approach is necessary.

IV. CAUSAL CONDITIONAL HEISENBERG DYNAMICS AS A WIENER FILTERING PROBLEM

The Heisenberg picture provides a framework for examining the dynamical evolution of quantum operators. In this section, we present a transformation from the Schrödinger picture to the Heisenberg picture within the context of SN-type nonlinear quantum mechanics. This transformation characterizes the evolution of the conditional quantum state as an optimal filtering problem.

In the causal conditional formalism, the conditional density matrix of the mechanical oscillator is expressed as [58, 60]:

$$\hat{\rho}_c = \langle y_N | \hat{U}_{N-1} \dots \hat{U}_1 \langle y_1 | \hat{U}_0 \hat{\rho}_0 \hat{U}_0^\dagger | y_1 \rangle \hat{U}_1^\dagger \dots \hat{U}_{N-1}^\dagger | y_N \rangle, \quad (25)$$

where $|y_i\rangle$ is the eigenvector of the outgoing light field and y_i is the optical phase measurement data. The $\hat{U}_i = \hat{U}(t_i, \langle x(t_i) \rangle_c)$ is the evolution operator of the time interval $[t_i, t_i + \Delta t]$ which depends on the conditional mean displacement, a hallmark of SN theory under causal conditional prescription. This density matrix can alternately be represented as:

$$\hat{\rho}_c = \text{Tr}_o[|y_N\rangle\langle y_N| \otimes \dots \otimes |y_1\rangle\langle y_1| \hat{U}_{N-1} \dots \hat{U}_0 \rho_0 \hat{U}_0^\dagger \dots \hat{U}_{N-1}^\dagger], \quad (26)$$

and in the continuous limit we have:

$$\hat{\rho}_c = \text{Tr}_o[\hat{\mathcal{P}} \hat{\mathcal{U}} \rho_0 \hat{\mathcal{U}}^\dagger] = \text{Tr}_o[\hat{\mathcal{U}} \rho_0 \hat{\mathcal{U}}^\dagger \hat{\mathcal{P}}], \quad (27)$$

where

$$\Pi_{i=1}^N \delta(\hat{y}_i - y_i) \rightarrow \int D[k(t')] \exp \left[i \int_{-\infty}^t dt' k(t') (\hat{y}(t) - y(t)) \right], \\ \hat{U}_{N-1} \dots \hat{U}_0 \rightarrow \hat{\mathcal{U}}(t, 0) = \mathcal{T} \left[\exp \left[-i \int_0^t dt' \hat{H}(\langle x(t') \rangle_c) \right] \right]. \quad (28)$$

The generating function is given by:

$$J(\alpha) = \text{Tr}_m[\hat{\rho}_c(t) e^{i\alpha\hat{x}}] = \text{Tr}[\hat{\mathcal{U}} \rho_0 \hat{\mathcal{U}}^\dagger \hat{\mathcal{P}} e^{i\alpha\hat{x}}]. \quad (29)$$

Utilizing the permutation symmetry in the trace operation and $\hat{\mathcal{U}}\hat{\mathcal{U}}^\dagger = 1$, we find:

$$J(\alpha) = \text{Tr}[\hat{\rho}_0 \hat{\mathcal{U}}^\dagger \hat{\mathcal{P}} \hat{\mathcal{U}} \hat{\mathcal{U}}^\dagger e^{i\alpha \hat{x}} \hat{\mathcal{U}}] = \text{Tr}[\hat{\rho}_0 \hat{\mathcal{P}}^H e^{i\alpha \hat{x}^H}], \quad (30)$$

where the Heisenberg picture operators are defined as:

$$\begin{aligned} e^{i\alpha \hat{x}^H(t)} &= \hat{\mathcal{U}}^\dagger(t, 0) e^{i\alpha \hat{x}} \hat{\mathcal{U}}(t, 0), \\ \hat{\mathcal{P}}^H &= \hat{\mathcal{U}}^\dagger(t, 0) \hat{\mathcal{P}} \hat{\mathcal{U}}(t, 0) \\ &= \int D[k(t')] \exp \left[i \int_{-\infty}^t dt' k(t') (\hat{y}^H(t) - y(t)) \right] \end{aligned} \quad (31)$$

This allows the generating function to be represented using Heisenberg picture operators, solvable via Heisenberg equations of motion in SN theory.

For a general theory with the classical-quantum mixture feature that (SN theory has such a feature as we shall see later):

$$\begin{aligned} \hat{y}^H(t) &= \hat{y}_q^H(t) + y_{\text{cl}}^H(t), \\ \hat{x}^H(t) &= \hat{x}_q^H(t) + x_{\text{cl}}^H(t), \end{aligned} \quad (32)$$

the generating functional is further formulated as:

$$\begin{aligned} J(\alpha) &= \exp \left[i\alpha x_{\text{cl}}^H(t) + i \int_{-\infty}^t dt' k(t') [y_{\text{cl}}^H(t') - y(t')] \right] \\ &\quad \int D[k(t')] \text{Tr} \left[\hat{\rho}_0 \exp \left(i\alpha \hat{x}_q^H(t) + i \int_{-\infty}^t dt' k(t') y_q^H(t') \right) \right]. \end{aligned} \quad (33)$$

The conditional density matrix thus becomes:

$$\begin{aligned} \hat{\rho}_c &= \text{Tr}_o[\hat{\mathcal{U}} \rho_0 \hat{\mathcal{U}}^\dagger \hat{\mathcal{P}}] = \text{Tr}_o[\rho_0 \hat{\mathcal{U}}^\dagger \hat{\mathcal{P}} \hat{\mathcal{U}}] = \text{Tr}_o[\rho_0 \hat{\mathcal{P}}^H] \\ &= \text{Tr}_o \left[\rho_0 \int D[k(t')] \exp \left[i \int_{-\infty}^t dt' k(t') (\hat{y}^H(t) - y(t)) \right] \right], \end{aligned} \quad (34)$$

and for a Gaussian process:

$$\begin{aligned} \text{Tr} \left[\hat{\rho}_0 \exp \left(i\alpha \hat{x}_q^H(t) + i \int_{-\infty}^t dt' k(t') y_q^H(t') \right) \right] \\ = \exp \left[-\frac{1}{2} \left\langle \left[\alpha \hat{x}_q^H(t) + \int_{-\infty}^t dt' k(t') y_q^H(t') \right]^2 \right\rangle \right], \end{aligned} \quad (35)$$

where $\langle \dots \rangle = \text{Tr}[\rho_0 \dots]$.

Expressing

$$\hat{x}_q^H(t) = \int_{-\infty}^t K_q(t-t') \hat{y}_q^H(t') dt' + \hat{R}(t), \quad (36)$$

with $\langle \hat{y}_q^H(t') \hat{R}(t) \rangle = 0, \forall t' < t$, meaning $K_q(t-t')$ is the optimal estimator of $\hat{x}_q(t)$ from the data string $y_q^H(t')$, results in:

$$\begin{aligned} -\frac{1}{2} \left\langle \left[\alpha \hat{x}_q^H(t) + \int_{-\infty}^t dt' k(t') y_q^H(t') \right]^2 \right\rangle &= \\ -\frac{1}{2} \left[\alpha \langle \hat{R}(t)^2 \rangle + \int \int dt' dt'' \tilde{K}(t, t') \tilde{K}(t, t'') \langle \hat{y}_q^H(t') \hat{y}_q^H(t'') \rangle \right], \end{aligned} \quad (37)$$

where the cross term $\propto \langle \hat{y}_q^H(t') \hat{R}(t) \rangle = 0$, and $\tilde{K}(t, t')$ is defined as:

$$\tilde{K}(t, t') = \alpha K_q(t-t') + k(t'). \quad (38)$$

Substituting the above equation into the generating functional yields:

$$\begin{aligned} J(\alpha) &= \exp \left[i\alpha x_{\text{cl}}^H(t) - \frac{1}{2} \alpha^2 \langle \hat{R}(t)^2 \rangle \right] \int D[k(t')] \\ &\quad \exp \left[i \int_{-\infty}^t dt' [\tilde{K}(t, t') - \alpha K_q(t-t')] [y_{\text{cl}}^H(t') - y(t')] \right] \\ &\quad \exp \left[-\frac{1}{2} \int \int dt' dt'' \tilde{K}(t, t') \tilde{K}(t, t'') \langle \hat{y}_q^H(t') \hat{y}_q^H(t'') \rangle \right]. \end{aligned} \quad (39)$$

Changing the functional variable:

$$\int D[k(t')] \rightarrow \int D[\tilde{K}(t, t')], \quad (40)$$

leads to

$$\begin{aligned} J(\alpha) &= \\ &\exp \left[i\alpha x_{\text{cl}}^H(t) - \frac{1}{2} \alpha^2 \langle \hat{R}(t)^2 \rangle - i\alpha \int_{-\infty}^t K_q(t-t') [y_{\text{cl}}^H(t') - y(t')] \right] \\ &\int D[\tilde{K}(t, t')] \left\langle \exp \left[i \int_{-\infty}^t dt' \tilde{K}(t, t') [\hat{y}^H(t') - y(t')] \right] \right\rangle, \end{aligned} \quad (41)$$

where the the following two equalities are used:

$$\begin{aligned} \left\langle \exp \left[i \int \tilde{K}(t, t') \hat{y}_q^H(t') dt' \right] \right\rangle &= \\ \exp \left[-\frac{1}{2} \int \int dt' dt'' \tilde{K}(t, t') \tilde{K}(t, t'') \langle \hat{y}_q^H(t') \hat{y}_q^H(t'') \rangle \right], \end{aligned} \quad (42)$$

$$\hat{y}^H(t') = \hat{y}_q^H(t') + \hat{y}_{\text{cl}}^H(t').$$

The functional integral in Eq. (41) is unity since it represents $\text{Tr}_m[\rho_c] = 1$.

Finally, the generation functional is:

$$\begin{aligned} J(\alpha) &= \exp \left[-\frac{1}{2} \alpha^2 \langle \hat{R}(t)^2 \rangle \right] \\ &\quad \exp \left[i\alpha x_{\text{cl}}^H(t) - i\alpha \int_{-\infty}^t K_q(t-t') [y_{\text{cl}}^H(t') - y(t')] \right] \end{aligned} \quad (43)$$

and the conditional mean is:

$$\langle \hat{x}(t) \rangle_c = \frac{\partial}{\partial \alpha} J(\alpha) \Big|_{\alpha=0} = x_{\text{cl}}^H(t) + \int_{-\infty}^t K_q(t-t') y_{\text{cl}}^H(t'), \quad (44)$$

where $y_q^H(t') \equiv y(t') - y_{\text{cl}}^H(t')$. The filter function $K_q(t-t')$ can be determined using the Wiener-Hopf method, familiar with standard quantum mechanics. This involves solving the Wiener-Hopf equation, $\langle \hat{y}_q^H(t') \hat{R}(t) \rangle = 0$:

$$C_{\hat{x}_q^H \hat{y}_q^H}(t, t') = \int_{-\infty}^t K_q(t-t') C_{\hat{y}_q^H \hat{y}_q^H}(t, t'), \quad \forall t' < t, \quad (45)$$

where $C_{\hat{A}\hat{B}}$ denotes the correlation function. As we will explore in the next section, within the SN theory, mechanical dynamics are partly driven by the conditional mean displacement $\langle x^H \rangle_c$ via classical gravity [22]. The Wiener filter method developed here allows for the calculation of $\langle x^H \rangle_c$, which is crucial for determining expressions for $\hat{x}^H(t)$ and the outgoing field quadrature data as influenced by mirror displacement. Given the relationship between the amplitude and phase quadratures of the incoming optical field and outgoing optical field quadrature at a homodyne detection angle θ in the Heisenberg picture, along with the known correlation of the amplitude and phase quadratures of the incoming field:

$$\langle \hat{a}_i(t) \hat{a}_j(t') \rangle_{\text{sym}} = \delta_{ij} \delta(t - t'), \quad (46)$$

where $\langle A(t) \hat{B}(t') \rangle_{\text{sym}} = \text{Tr}[\hat{\rho}(\langle A(t) \hat{B}(t') + \langle B(t') \hat{A}(t) \rangle)/2]$ defines the correlation function for two Hermitian operators \hat{A}, \hat{B} , and $(i, j = 1, 2)$ denote the amplitude and phase quadratures, it becomes straightforward to compute the correlation spectrum for any two outgoing optical field quadratures. This computation subsequently facilitates the calculation of logarithmic negativity.

V. HEISENBERG-PICTURE APPROACH TO THE OPTOMECHANICAL PROTOCOLS

In the previous section, we can see that one key step in obtaining the filter function $K_q(t - t')$ is to compute the correlation function of \hat{x}_q^H, \hat{y}_q^H , which means we need to find the expression of the displacement/field quadrature decomposition $\hat{x}^H = \hat{x}_q^H + x_{\text{cl}}^H, \hat{y}^H = \hat{y}_q^H + y_{\text{cl}}^H$. For brevity, we will omit all superscripts H of the operators in the following text, since we are working in the Heisenberg picture. The expressions of $\hat{x}(t), \hat{y}(t)$ can be obtained by solving the Heisenberg equations of motion for the mechanical oscillator in the SN theory:

$$\begin{aligned} \dot{\hat{x}} &= \frac{\hat{p}}{M}, \\ \dot{\hat{p}} &= -M(\omega_m^2 + \omega_{SN}^2)\hat{x} + M\omega_{SN}^2\langle \hat{x} \rangle_c + \hbar\alpha\hat{a}_1. \end{aligned} \quad (47)$$

Here, the SN gravity potential affects the test mass in two ways: (1) it shifts the resonant frequency of \hat{x} from ω_m to $\omega_q = \sqrt{\omega_m^2 + \omega_{SN}^2}$; (2) within the causal-conditional formalism, there is an interpretation where a "spectator," aware of all measurement records, applies the self-gravity force $M\omega_{SN}^2\langle \hat{x} \rangle_c$ on the test mass.

The input-output relation for the optical field is:

$$\hat{b}_\theta = \cos \theta \hat{a}_1 + \sin \theta \hat{a}_2 + \sin \theta \alpha \hat{x}. \quad (48)$$

The solution of Eq.(47) is:

$$\hat{x}(t) = \int_{-\infty}^t dt' \chi_q(t - t')[\alpha \hat{a}_1(t') + M\omega_{SN}^2 \langle \hat{x}(t') \rangle_c], \quad (49)$$

where χ_q is the quantum mechanical response function with Fourier-transformed form as

$$\chi_q(\omega) = \frac{1}{m(-\omega^2 + \omega_q^2 - i\gamma_m \omega)}. \quad (50)$$

This $\hat{x}(t)$ can be decomposed as

$$\begin{aligned} \hat{x}(t) &= \hat{x}_q(t) + x_{\text{cl}}(t), \\ \hat{x}_q(t) &= \int_{-\infty}^t dt' \chi_q(t - t') \alpha \hat{a}_1(t'), \\ x_{\text{cl}}(t) &= \int_{-\infty}^t dt' \chi_q(t - t') M\omega_{SN}^2 \langle \hat{x}(t') \rangle_c. \end{aligned} \quad (51)$$

The $\hat{x}_q(t)$ is the displacement operator driven by the environmental quantum noise (e.g. radiation pressure noise), and $x_{\text{cl}}(t)$ is a classical displacement driven by the classical gravity sourced by conditional mean displacement $\langle \hat{x}(t') \rangle_c$ for $t' < t$.

Substituting the solution of Eq.(47) into the above input-output relation leads to:

$$\begin{aligned} \hat{b}_\theta(t) &= \cos \theta \hat{a}_1 + \sin \theta \hat{a}_2 + \sin \theta \alpha \int_{-\infty}^t \chi_q(t - t') \hbar \hat{a}_1(t') dt' \\ &\quad + \sin \theta \alpha \int_{-\infty}^t \chi_q(t - t') M\omega_{SN}^2 \langle \hat{x}(t') \rangle_c dt', \end{aligned} \quad (52)$$

where the field quadrature with homodyne angle θ is measured, and this \hat{b}_θ corresponds to the $\tilde{y}_q^H(t)$ in the previous section. Measuring the outgoing field $\hat{b}_\theta(t)$ yields a data string \tilde{y}_θ (which indicates the commutation relation $[\hat{b}_\theta(t), \hat{b}_\theta(t')] = 0$). This data string \tilde{y}_θ comprises two components: the term from the classical conditional mean mechanical displacement $\langle \hat{x}(t) \rangle_c$, and the quantum term $y_\theta^q(t)$:

$$\hat{b}_\theta^q(t) = \hat{b}_\theta(t) - \sin \theta \alpha \int_{-\infty}^t \chi_q(t - t') M\omega_{SN}^2 \langle \hat{x}(t') \rangle_c dt', \quad (53)$$

which also satisfies $[\hat{b}_\theta^q(t), \hat{b}_\theta^q(t')] = 0$.

A. Causal-conditional dynamics as a Wiener filtering problem

Following the discussion in Section IV, we now analyse the causal-conditional dynamics in SN theory as a Wiener filtering problem [58, 61, 62].

Substituting the formulae of $\hat{b}_\theta^q(t), \hat{x}_q(t)$ into the Wiener-

Hopf equation (45), we can obtain the Wiener filter function

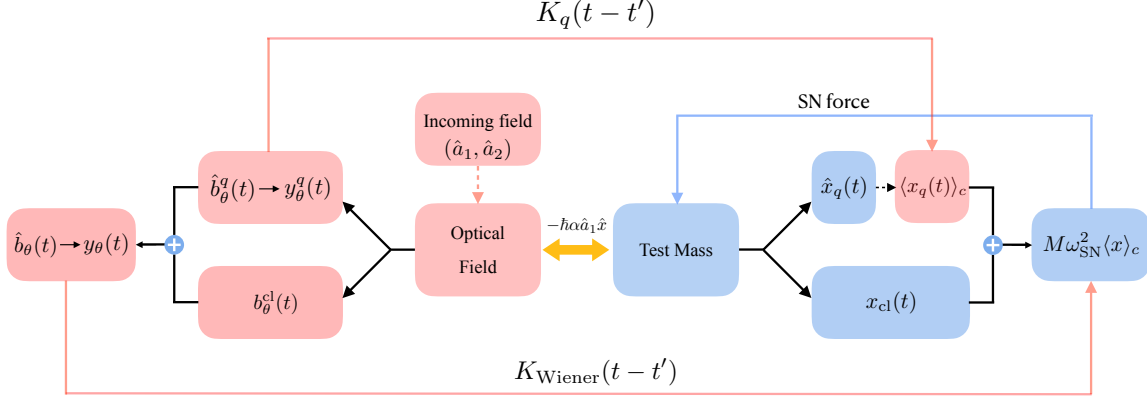


FIG. 3. In the Heisenberg picture, causal conditional dynamics can be approached as a Wiener filtering problem, particularly within the self-gravity protocol of the SN theory. Here, the conditional displacement of the test mass, $\langle x(t) \rangle_c$, is composed of two distinct components. The first component arises from the quantum radiation pressure force and can be determined by filtering the quantum component of the outgoing field \hat{b}_θ^q . The second component is a result of the classical gravity force, which is influenced by the quantum trajectory $\langle x(t') \rangle_c$ at earlier times $t < t'$. The accompanying flowchart outlines the method for calculating these causal conditional dynamics, as detailed in the main text. Note that the $\langle x_q(t) \rangle_c$ is obtained through Wiener-filtering the optical data, which provides an optimal estimation of the $\hat{x}_q(t)$. This is why the $\langle x_q(t) \rangle_c$ is represented in pink.

$K_q(\Omega)$ in the frequency domain using the famous Wiener-Hopf method (for a detailed derivation, see Appendix):

$$\begin{aligned} K_q(\Omega) &= \frac{\beta\beta_c + \Omega(\beta - \beta_c) + i\gamma_m\Omega - \omega_m^2}{\alpha \sin \theta (\beta - \Omega)(\Omega + \beta_c)} \\ &= \frac{A_q^\theta(\Omega)}{\alpha \sin \theta (A_q^\theta(\Omega) - R_q(\Omega))}, \end{aligned} \quad (54)$$

where $R_q(\Omega) = \omega_q^2 - \Omega^2 - i\gamma_m\Omega$ and $A_q^\theta(\Omega)$ has the same form as Eq. (21). In the first line, $\beta = \beta_c^*$ are the roots of the numerator of the spectrum $S_{y_\theta^q y_\theta^q}$. Detailed expressions for these roots are provided in Appendix A 1 (note that the ω_m in Appendix A 1 should be replaced by ω_q in the SN theory). The validity of the second equality is demonstrated in Appendix A 2.

Using Eq. (44):

$$\begin{aligned} \langle x(t) \rangle_c &= \int_{-\infty}^t dt' K_q(t-t') \tilde{y}_\theta^q(t') \\ &\quad + \int_{-\infty}^t dt' \chi_q(t-t') M \omega_{SN}^2 \langle \hat{x}(t') \rangle_c, \end{aligned} \quad (55)$$

and applying a Fourier transformation leads to the conditional mean displacement in the frequency domain $\langle x(\Omega) \rangle_c$:

$$\langle \hat{x}(\Omega) \rangle_c = \frac{\chi_m(\Omega)}{\chi_q(\Omega)} K_q(\Omega) \tilde{y}_\theta^q(\Omega). \quad (56)$$

When overviewing the Schrödinger-picture approach, we have derived the filter function using an alternative method based on the master equation (7). To facilitate a comparison between these two approaches, we require another form of the

filter function that relates the conditional mean displacement $\langle \hat{x}(\Omega) \rangle_c$ to the complete data string $\tilde{y}_\theta(\Omega)$. By representing the $\tilde{y}_\theta(\Omega)$ in terms of $\langle \hat{x}(\Omega) \rangle_c$ using Eq. (56) and substituting into:

$$\tilde{y}_\theta(\Omega) = \tilde{y}_\theta^q(\Omega) + \sin \theta \alpha \chi_q(\Omega) M \omega_{SN}^2 \langle x(\Omega) \rangle_c, \quad (57)$$

leads to a filter function $K_{\text{Wiener}}(\Omega)$:

$$\begin{aligned} \langle \hat{x}(\Omega) \rangle_c &= K_{\text{Wiener}}(\Omega) \tilde{y}_\theta(\Omega), \\ K_{\text{Wiener}}(\Omega) &= \frac{A_q^\theta(\Omega)}{\alpha \sin \theta (A_q^\theta(\Omega) - R_m(\Omega))}, \end{aligned} \quad (58)$$

where $A_q^\theta(\Omega)$ and $R_m(\Omega)$ are given in Eqs. (13). This filter function is the same as the $K_\theta(\Omega)$ (Eq.(21)) derived in the Schrödinger picture.

Complementary, if we directly substitute Eq. (56) into Eq. (57), we can rewrite Eq. (57) in terms of \tilde{y}_θ^q and finally compute the covariance matrix of the outgoing light field which will be discussed in Section V B.

B. Spectrum and covariance matrix for the outgoing field

Utilizing the filter function to compute the conditional mean motion in the SN theory enables the calculation of the covariance matrix for the outgoing field.

The measurement record \tilde{y}_θ can be expressed as:

$$\tilde{y}_\theta(\Omega) = \tilde{y}_\theta^q(\Omega) + M \omega_{SN}^2 \sin \theta \alpha \chi_q(\Omega) K_{\text{Wiener}}(\Omega) \tilde{y}_\theta(\Omega). \quad (59)$$

By substituting the Wiener filter $K_{\text{Wiener}}(\Omega)$ into Eq.(58), we obtain:

$$\tilde{y}_\theta(\Omega) = K_{yy}^\theta(\Omega) \tilde{y}_\theta^q(\Omega),$$

$$\text{where } K_{yy}^\theta(\Omega) = \frac{R_q(\Omega)}{R_m(\Omega)} \frac{A_q^\theta(\Omega) - R_m(\Omega)}{A_q^\theta(\Omega) - R_q(\Omega)}. \quad (60)$$

The noise spectrum of the outgoing field is then computed as:

$$S_{\tilde{y}_\theta \tilde{y}_\theta}(\Omega) = \left| K_{yy}^\theta(\Omega) \right|^2 S_{\tilde{y}_\theta^q \tilde{y}_\theta^q}(\Omega), \quad (61)$$

where $S_{\tilde{y}_\theta^q \tilde{y}_\theta^q}(\Omega)$ is given by the standard optomechanical system:

$$S_{\tilde{y}_\theta^q \tilde{y}_\theta^q}(\Omega) = 1 + \alpha^2 \sin 2\theta \text{Re}[\chi_q(\Omega)] + \alpha^4 \sin^2 \theta |\chi_q(\Omega)|^2. \quad (62)$$

Appendix B demonstrates that $S_{\tilde{y}_\theta^q \tilde{y}_\theta^q}(\Omega)$ satisfies the equality:

$$S_{\tilde{y}_\theta^q \tilde{y}_\theta^q}(\Omega) = \left| \frac{A_q^\theta(\Omega) - R_q(\Omega)}{R_q(\Omega)} \right|^2. \quad (63)$$

Thus, we deduce:

$$S_{\tilde{y}_\theta \tilde{y}_\theta}(\Omega) = \left| \frac{A_q^\theta(\Omega) - R_m(\Omega)}{R_m(\Omega)} \right|^2, \quad (64)$$

which is exactly equivalent to the result we obtained using the Schrödinger picture in Eq.(12) in Section II.

In addition, the environmental effect needs to be considered in the calculation of the spectrum and covariance matrix. Within the framework of nonlinear quantum mechanical theories, there are two different prescriptions to treat the thermal environment, and this subtlety was extensively discussed in [22]. Generally speaking, these two prescriptions correspond to treating the thermal noise classically or quantum-mechanically. In the main text, we focus on quantum thermal noise, while classical thermal noise is discussed in detail in the Appendix C. Quantum thermal noise in this context includes all unmonitored environmental noise sources that lead to decoherence of the quantum state. This interpretation treats environmental degrees of freedom as part of the quantum mechanical system. The quantum thermal noise drives the quantum motion of the test mass and affects the outgoing optical quadrature as,

$$\hat{b}_\theta^q(t) = \cos \theta \hat{a}_1 + \sin \theta \hat{a}_2 + \sin \theta \alpha \int_{-\infty}^t \chi_q(t-t') \hbar \hat{a}_1(t') dt'$$

$$+ \sin \theta \alpha \int_{-\infty}^t \chi_q(t-t') \hat{F}_{\text{th}} dt', \quad (65)$$

The thermal noise spectrum approximation at high-temperature is:

$$S_{F_{\text{th}} F_{\text{th}}}(\Omega) = 4\hbar \left[\frac{1}{e^{\frac{\hbar\Omega}{k_B T}} - 1} + \frac{1}{2} \right] \frac{\text{Im}[\chi_m(\Omega)]}{|\chi_m(\Omega)|^2} \quad (66)$$

$$\approx 4k_B T M \gamma_m + 2\hbar \Omega M \gamma_m.$$

The quantum thermal noise modifies the Wiener filter function, in which the factor a_2 of the β (details in Appendix A.1) is modified as:

$$a_2 = 2\tilde{\Lambda}^4(1 - \cos 2\theta) + 4\omega_q^2(\omega_q^2 + \Lambda^2 \sin 2\theta) \quad (67)$$

where $\tilde{\Lambda}^2 = \Lambda^2 + 4\gamma_m k_B T / \hbar$.

Since the mathematical structure of the above formulas is unchanged by the thermal noise, the filter function $K_q(\Omega)$ is also formally unchanged. Then it is easy to show that the $S_{\tilde{y}_\theta \tilde{y}_\theta}$ also takes the same form, except that the β substituted in $A_q^\theta(\Omega)$ (seen Appendix.B) should be given by the above formula Eq.(67). Straightforward algebra shows that the outgoing field with the contribution of a quantum thermal bath is:

$$\begin{aligned} S_{\tilde{y}_\theta \tilde{y}_\theta} = & 1 + |\chi_m|^2 \alpha^4 \sin^4 \theta + |\chi_m|^2 \alpha^2 \sin 2\theta (\omega_m^2 - \Omega^2) \\ & + 4|\chi_m|^2 \sin \theta^2 \alpha^2 M \gamma_m k_B T \\ & + \omega_{\text{SN}}^2 M^2 |\chi_m|^2 [2\omega_q^2 + \Lambda^2 \sin 2\theta \\ & - 2\sqrt{\Lambda^2 \tilde{\Lambda}^2 \sin^2 \theta + \omega_q^2(\omega_q^2 + 2\Lambda^2 \sin 2\theta)}]. \end{aligned} \quad (68)$$

The components of this spectrum have transparent physical meaning: the first line accounts for quantum shot noise and back-action noise [3], the second line arises from the thermal bath's direct impact on \hat{x} -dynamics, and the final two lines describe the effect of classical self-gravity (SN term) modified by the quantum thermal bath. Basically, the evolution of the $\langle \hat{x}(t) \rangle_c$ depends on V_{xx} , which is affected by the thermal bath. Consequently, the self gravity force $-M\omega_{\text{SN}}^2 \langle \hat{x}(t) \rangle_c$, which drives the test mass, is also affected by the thermal bath. The spectrum $S_{\tilde{y}_\theta \tilde{y}_\theta}$ can also be derived using the Wiener filter method.

Parameters	Symbol	Value
Mirror mass	M	0.2 kg
Mirror bare frequency	$\omega_m/(2\pi)$	4×10^{-3} Hz
SN frequency	$\omega_{\text{SN}}/(2\pi)$	7.8×10^{-2} Hz
Quality factor	Q_m	10^7
Mechanical damping	$\gamma_m/(2\pi)$	4×10^{-10} Hz
Optical wavelength	λ	1064 nm
Cavity Finesse	\mathcal{F}	300
Intra-cavity power	P_{cav}	480 nW

TABLE I. Sample parameters for the self-gravity optomechanical protocol.

Considering the thermal bath, we can also compute the cross-correlation function using Eq.(60). The resulting covariance matrix is:

$$\mathbf{V}(\Omega) = \begin{bmatrix} S_{\tilde{y}_0^q \tilde{y}_0^q}(\Omega) & K_{yy}^{\pi/2*}(\Omega) S_{\tilde{y}_{\pi/2}^q \tilde{y}_0^q}(\Omega) \\ K_{yy}^{\pi/2}(\Omega) S_{\tilde{y}_0^q \tilde{y}_{\pi/2}^q}(\Omega) & \left| K_{yy}^{\pi/2}(\Omega) \right|^2 S_{\tilde{y}_{\pi/2}^q \tilde{y}_{\pi/2}^q}(\Omega) \end{bmatrix}, \quad (69)$$

where $S_{\tilde{y}_0^q \tilde{y}_0^q}(\Omega) = 1$, $S_{\tilde{y}_0^q \tilde{y}_{\pi/2}^q}(\Omega) = S_{\tilde{y}_{\pi/2}^q \tilde{y}_0^q}^*(\Omega) = \alpha^2 \chi_q(\Omega)$ and $S_{\tilde{y}_{\pi/2}^q \tilde{y}_{\pi/2}^q}(\Omega) = 1 + \alpha^4 |\chi_q(\Omega)|^2 + 4\alpha^2 |\chi_q(\Omega)|^2 M \gamma_m k_B T$. The

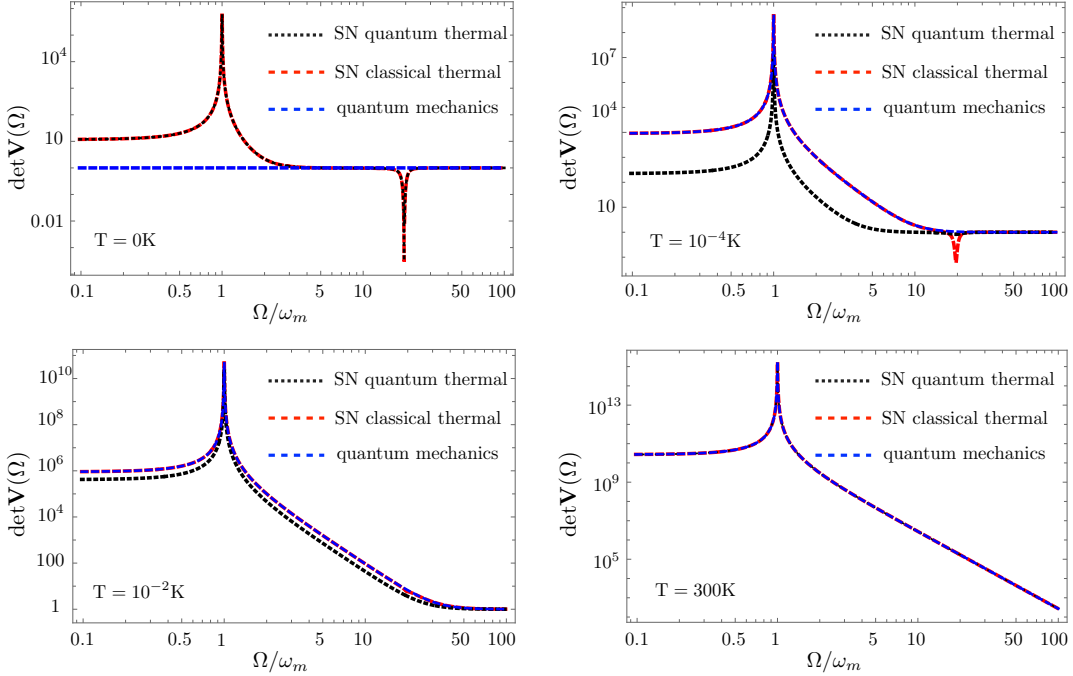


FIG. 4. The $\det\mathbf{V}(\Omega)$ at different temperatures of SN theory and quantum gravity for the self-gravity protocol. Note that the $\det\mathbf{V}(\Omega)$ can be smaller than one in the SN case when the temperature is sufficiently low. When $T = 0$, the dip of $\det\mathbf{V}(\Omega)$ in the SN case locates at $\Omega = \omega_q$, which originates from the factor $K_{yy}^{\pi/2}(\Omega)$. We plot three different cases, the black and red curves are the $\det\mathbf{V}(\Omega)$ in the SN theory where the thermal noise is treated quantum mechanically and classically, while the blue curve is the $\det\mathbf{V}(\Omega)$ in standard quantum mechanics. The details of classical thermal noise are discussed in Appendix C.

determinant of this covariance matrix is

$$\det\mathbf{V}(\Omega) = \left|K_{yy}^{\pi/2}(\Omega)\right|^2 (1 + 4\alpha^2 |\chi_q(\Omega)|^2 M \gamma_m k_B T), \quad (70)$$

where $\det\mathbf{V}(\Omega) = 1$ in standard quantum mechanics ($K_{yy}^{\pi/2}(\Omega) = 1$ since $R_q(\Omega) \rightarrow R_m(\Omega)$) with $T = 0$. With sample parameters in Tab. I, we plot the $\det\mathbf{V}(\Omega)$ in Fig. 4, which reveals that $\det\mathbf{V}(\Omega)$ can be less than one in the SN scenario at sufficiently low temperatures (in particular at $\Omega = \omega_q$), challenging the usual expectation of $\det\mathbf{V}(\Omega) \geq 1$ for pure and mixed states.

In standard quantum mechanics, the Heisenberg uncertainty principle dictates that the covariance matrix of the outgoing field satisfies $\det[\mathbf{V}] \geq 1$ or $S_{b_1 b_1} S_{b_2 b_2} - |S_{b_1 b_2}|^2 \geq$

1 [63], reflecting that the optical field exchanges no net energy with the test mass. In the context of SN theory, however, when $\det\mathbf{V}(\Omega) < 1$, this does not imply a violation of Heisenberg's principle. This is substantiated by the fact that both commutators, $[\hat{b}, \hat{b}^\dagger] = 1$ and $[\hat{b}^q, \hat{b}^{q\dagger}] = 1$, preserve the unitarity condition. Therefore, the covariance matrix under discussion does not precisely represent the quantum state of the light. The fundamental difference from quantum gravity is that \hat{b} in SN theory is a quantum-classical mixed operator, incorporating a classical component from the SN term. Indeed, it is the covariance matrix of \tilde{y}_θ^q , rather than \tilde{y}_θ , that maintains the Heisenberg uncertainty principle by excluding the averaging over the SN term influenced by quantum trajectories.

Furthermore, the Wigner function of the outgoing field can be obtained from the covariance matrix in standard quantum optomechanics, which is called *optical state tomography* [64, 65]. For a Gaussian state, the cross-section of the Wigner function is an ellipse in the phase space of the optical state [66], which can be determined by the optical quadrature spectrum measured at three different homodyne angles. The foundation of this state tomography process is that, in standard quantum mechanics, different homodyne measurement

angles correspond to the same state evolution. However, in the SN theory, measurements at different homodyne angles lead to different quantum trajectories, which source different evolution of the self-gravity potential and hence different mirror and optical state evolution. Therefore, although Heisenberg picture analysis allows us to compute the covariance matrix in a similar way as standard quantum mechanics, the state tomography process in SN theory is subtle due to the intrinsic SN nonlinearity. Such a subtlety will also appear in the mutual

gravity protocol as we shall see in the later sections.

VI. MUTUAL GRAVITY PROTOCOL AND ENTANGLEMENT

In this section, we explore the mutual gravity protocol to test the quantum nature of gravity [19]. In particular, we further investigate the optical correlation in these experiments, and demonstrate that this correlation will constitute apparent entanglement that will be a false alarm of quantum gravity signature. In this setup, two optical fields, strengthened by cavities, track two test mass mirrors, which interact through mutual gravity. The equations describing the system's dynamics are given by:

$$\begin{aligned}\dot{\hat{x}}_{A/B} &= \frac{\hat{p}_{A/B}}{M}, \\ \dot{\hat{p}}_{A/B} &= -M\omega_q^2 \hat{x}_A - \gamma_m \hat{p}_A + M\omega_g^2 \langle \hat{x}_{B/A} \rangle_c + \alpha \hat{a}_{1A/B}, \\ \hat{b}_{\theta A/B} &= \sin \theta \hat{a}_{2A/B} + \cos \theta \hat{a}_{1A/B} + \sin \theta \alpha \hat{x}_{A/B},\end{aligned}\quad (71)$$

where $\omega_g = \sqrt{2\mathcal{C}/M}$ and $\omega_q^2 = \omega_m^2 - \omega_g^2$.

Solving these motion equations results in:

$$\begin{aligned}\hat{b}_{\theta A/B}(t) &= \cos \theta \hat{a}_{1A/B} + \sin \theta \hat{a}_{2A/B} \\ &+ \sin \theta \alpha \int_{-\infty}^t \chi_q(t-t') (\hbar \hat{a}_{1A/B}(t') + 2\mathcal{C} \langle \hat{x}_{B/A}(t') \rangle_c) dt',\end{aligned}\quad (72)$$

where the quantum contribution $\hat{b}_{\theta A/B}$ is defined by:

$$\begin{aligned}\hat{b}_{\theta A/B}^q &= \cos \theta \hat{a}_{1A/B} + \sin \theta \hat{a}_{2A/B} \\ &+ \sin \theta \alpha \int_{-\infty}^t \chi_q(t-t') \hbar \hat{a}_{1A/B}(t') dt',\end{aligned}\quad (73)$$

and the projective measurement data of the outgoing light is:

$$\begin{aligned}\tilde{y}_{\theta A/B}(t) &= \tilde{y}_{\theta A/B}^q(t) \\ &+ 2\mathcal{C} \sin \theta \alpha \int_{-\infty}^t \chi_q(t-t') \langle \hat{x}_{B/A}(t') \rangle_c dt',\end{aligned}\quad (74)$$

For illustration, consider $\theta_A = \theta_B = \theta$. The frequency domain expression for $K_q^{A/B}(\Omega)$ is:

$$K_q^{A/B}(\Omega) = \frac{\beta \beta_c + \Omega(\beta - \beta_c) + i\gamma_m \Omega - \omega_m^2}{\alpha \sin \theta (\beta - \Omega)(\Omega + \beta_c)}. \quad (78)$$

In the frequency domain, the conditional displacement of mirror A/B is:

$$\langle \hat{x}_{A/B}(\Omega) \rangle = K_q^{A/B}(\Omega) \tilde{y}_{\theta A/B}^q(\Omega) + M\omega_g^2 \chi_q(\Omega) \langle \hat{x}_{A/B}(\Omega) \rangle, \quad (79)$$

where $\tilde{y}_{\theta AB}^q$ pertains to the projective measurement data on $\hat{b}_{\theta AB}^q$. The primary challenge in the causal conditional prescription is extracting $\langle \hat{x}_{A/B} \rangle_c$ from $\tilde{y}_{\theta AB}$, which will be addressed using both the stochastic master equation filter method and the Wiener filter method.

A. Filter functions

1. Wiener filter approach

Following the procedure established for the self-gravity protocol, the displacement $\hat{x}(t)$ can be expressed as:

$$\hat{x}_{A/B}(t) = \int_{-\infty}^t \chi_q(t-t') (\hbar \alpha \hat{a}_{1A/B}(t') + M\omega_g^2 \langle \hat{x}_{B/A}(t') \rangle_c) dt'. \quad (75)$$

We separate $\hat{x}_{A/B}$ into $x_{A/B}^c$ and $\hat{x}_{A/B}^q$:

$$\begin{aligned}\hat{x}_{A/B}^q(t) &= \int_{-\infty}^t dt' \chi_q(t-t') \hbar \alpha \hat{a}_{1A/B}(t'), \\ x_{A/B}^c(t) &= M\omega_g^2 \int_{-\infty}^t dt' \chi_q(t-t') \langle \hat{x}_{B/A}(t') \rangle_c.\end{aligned}\quad (76)$$

Thus, $\langle \hat{x}_{A/B}^q \rangle \equiv \langle \hat{x}_{A/B}^q \rangle_c - x_{A/B}^c$ is related to $\tilde{y}_{\theta A/B}^q$ via the Wiener filter $K_q^{A/B}(t-t')$:

$$\langle \hat{x}_{A/B}^q(t) \rangle = \int_{-\infty}^t K_q^{A/B}(t-t') \tilde{y}_{\theta A/B}^q(t') dt'. \quad (77)$$

In the SN theory's causal-conditional framework, the left and right optomechanical systems interact solely via the mutual gravitational influence of quantum trajectories.

Therefore, $\tilde{y}_{\theta A/B}^q$ is akin to the self-gravity protocol, aside from the modification of the resonance frequency by mutual gravity.

which leads to

$$\begin{aligned}\langle \hat{x}_{A/B}(\Omega) \rangle &= \frac{R_q^2(\Omega)}{R_+(\Omega) R_-(\Omega)} K_q^{A/B}(\Omega) \tilde{y}_{\theta A/B}^q(\Omega) \\ &+ \frac{\omega_g^2(\Omega) R_q(\Omega)}{R_+(\Omega) R_-(\Omega)} K_q^{B/A}(\Omega) \tilde{y}_{\theta B/A}^q(\Omega).\end{aligned}\quad (80)$$

Substituting into the output measurement data:

$$\tilde{y}_{\theta A/B}(\Omega) = \tilde{y}_{\theta A/B}^q(\Omega) + \frac{M\omega_g^2 \sin \theta \alpha}{R_q(\Omega)} \langle \hat{x}_{B/A} \rangle(\Omega), \quad (81)$$

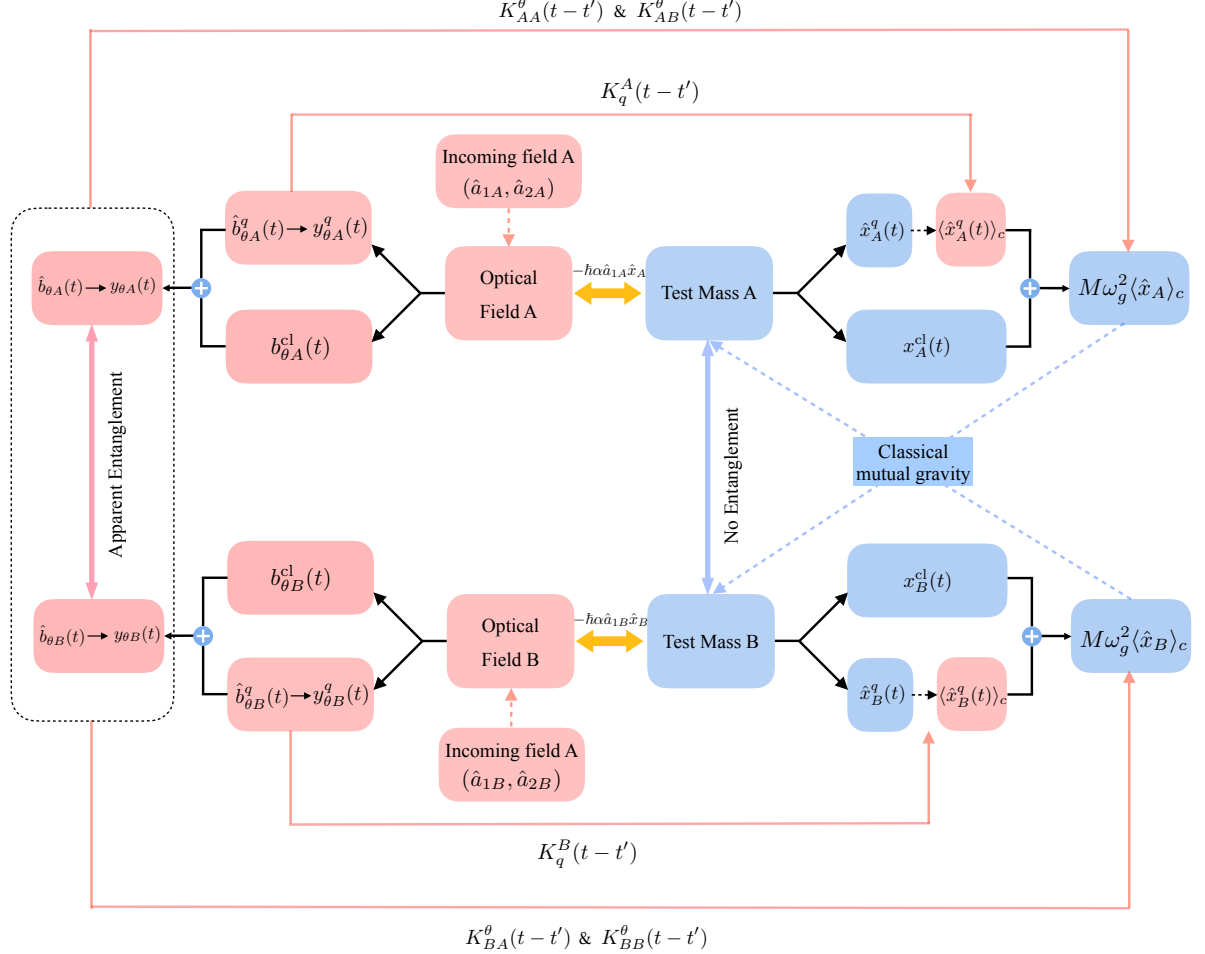


FIG. 5. Causal conditional dynamics as a Wiener filtering problem in the Heisenberg picture for the mutual-gravity protocol. In SN theory, the test masses interact through classical gravity, characterized by the c-number terms $M\omega_g^2\langle\hat{x}_{A/B}\rangle_c$. This implies that the quantum states of test masses A and B are not entangled. The appearance of apparent entanglement between the two outgoing fields arises from the interaction of the quantum trajectories of the test masses.

yields:

$$\tilde{y}_{\theta A/B}(\Omega) = \left[1 + \frac{\alpha \sin \theta \omega_g^4 K_q^{A/B}(\Omega)}{R_+(\Omega) R_-(\Omega)} \right] \tilde{y}_{\theta A/B}^q(\Omega) + \left[\frac{\alpha \sin \theta \omega_g^2 R_q(\Omega) K_q^{B/A}(\Omega)}{R_+(\Omega) R_-(\Omega)} \right] \tilde{y}_{\theta B/A}^q(\Omega). \quad (82)$$

For the special case $\theta = \pi/2$:

$$\tilde{y}_{2A/B}(\Omega) = \left[1 + \frac{\alpha \omega_g^4 K_{q,\pi/2}^{A/B}(\Omega)}{R_+(\Omega) R_-(\Omega)} \right] \tilde{y}_{2A/B}^q(\Omega) + \left[\frac{\alpha \omega_g^2 R_q(\Omega) K_{q,\pi/2}^{B/A}(\Omega)}{R_+(\Omega) R_-(\Omega)} \right] \tilde{y}_{2B/A}^q(\Omega). \quad (83)$$

By employing Eq. (78), we find:

$$\begin{aligned} \tilde{y}_{2A/B}(\Omega) = & \\ & \left[1 + \frac{\omega_g^4}{R_+(\Omega) R_-(\Omega)} \frac{(\beta - \Omega)(\beta_c + \Omega) - R_m(\Omega)}{(\beta - \Omega)(\beta_c + \Omega)} \right] \tilde{y}_{2A/B}^q(\Omega) \\ & + \left[\frac{\omega_g^2 R_q(\Omega)}{R_+(\Omega) R_-(\Omega)} \frac{(\beta - \Omega)(\beta_c + \Omega) - R_m(\Omega)}{(\beta - \Omega)(\beta_c + \Omega)} \right] \tilde{y}_{2B/A}^q(\Omega). \end{aligned} \quad (84)$$

Calculations in Appendix A.2 confirm that $\tilde{y}_{2A/B}(\Omega)$ (Eq.(84)) matches precisely with the result obtained by the stochastic master equation method (Eq.(91)).

2. Stochastic Master equation approach

Firstly, we calculate the filter function based on the long-term behavior of the stochastic master equation. To extract $\langle \hat{x}_{A/B} \rangle_c$ from $\tilde{y}_{\theta A/B}$, assuming $\theta = \pi/2$, we propose a two-channel filter matrix:

$$\begin{bmatrix} \langle \hat{x}_A(t) \rangle_c \\ \langle \hat{x}_B(t) \rangle_c \end{bmatrix} = \int_{-\infty}^t dt' \begin{bmatrix} K_{AA}(t-t') & K_{AB}(t-t') \\ K_{BA}(t-t') & K_{BB}(t-t') \end{bmatrix} \begin{bmatrix} \tilde{y}_{2A}(t') \\ \tilde{y}_{2B}(t') \end{bmatrix}. \quad (85)$$

Solving these filter functions involves the evolution equations of the conditional expectation value $\langle \hat{x}_{A/B} \rangle_c$:

$$d \begin{bmatrix} \langle \hat{x}_A \rangle_c \\ \langle \hat{p}_A \rangle_c \\ \langle \hat{x}_B \rangle_c \\ \langle \hat{p}_B \rangle_c \end{bmatrix} = \mathbb{M} \begin{bmatrix} \langle \hat{x}_A \rangle \\ \langle \hat{p}_A \rangle \\ \langle \hat{x}_B \rangle \\ \langle \hat{p}_B \rangle \end{bmatrix} + 2\alpha \begin{bmatrix} V_{xx}^A \tilde{y}_{2A} \\ V_{xp}^A \tilde{y}_{2A} \\ V_{xx}^B \tilde{y}_{2B} \\ V_{xp}^B \tilde{y}_{2B} \end{bmatrix}, \quad (86)$$

where

$$\mathbb{M} = \begin{bmatrix} -2\alpha^2 V_{xx}^A & 1/M & 0 & 0 \\ -M\omega_q^2 - 2\alpha^2 V_{xp}^A & -\gamma_m & M\omega_g^2 & 0 \\ 0 & 0 & -2\alpha^2 V_{xx}^B & 1/M \\ M\omega_g^2 & 0 & -M\omega_q^2 - 2\alpha^2 V_{xp}^B & -\gamma_m \end{bmatrix} \quad (87)$$

and we have reexpress all $dW_{A/B}$ in terms of $\tilde{y}_{\theta A/B}$.

In a symmetric configuration, where both optomechanical cavities have matching parameters, we have $V_{xx}^A = V_{xx}^B = V_{xx}$ and $V_{xp}^A = V_{xp}^B = V_{xp}$. By solving Eq.(86), the two-channel filter function in the frequency domain is:

$$\begin{aligned} K_{AA/BB}(\Omega) &= \frac{A(\Omega)}{\alpha(2A(\Omega) + R^-(\Omega))} + \frac{A(\Omega)}{\alpha(2A(\Omega) + R^+(\Omega))}, \\ K_{AB/BA}(\Omega) &= \frac{A(\Omega)}{\alpha(2A(\Omega) + R^-(\Omega))} - \frac{A(\Omega)}{\alpha(2A(\Omega) + R^+(\Omega))}, \end{aligned} \quad (88)$$

where

$$\begin{aligned} A(\Omega) &= V_{xx}\alpha^2(V_{xx}\alpha^2 + \gamma_m - i\Omega), \\ R^-(\Omega) &= \omega_q^2 - \omega_g^2 - \Omega^2 - i\gamma_m\Omega, \\ R^+(\Omega) &= \omega_q^2 + \omega_g^2 - \Omega^2 - i\gamma_m\Omega. \end{aligned} \quad (89)$$

The frequency domain measurement record, as stated in Eq.(74), is now:

$$\begin{bmatrix} \tilde{y}_{2A}(\Omega) \\ \tilde{y}_{2B}(\Omega) \end{bmatrix} = \left[\mathbf{1} - M\omega_g^2 \alpha \chi_q(\Omega) \begin{pmatrix} K_{BA}(\Omega) & K_{BB}(\Omega) \\ K_{AA}(\Omega) & K_{AB}(\Omega) \end{pmatrix} \right]^{-1} \begin{bmatrix} \tilde{y}_{2A}^q(\Omega) \\ \tilde{y}_{2B}^q(\Omega) \end{bmatrix}. \quad (90)$$

This simplifies to:

$$\begin{aligned} \tilde{y}_{2A/B} &= \left[1 + \frac{2\omega_g^2}{R^+(\Omega)R^-(\Omega)} \frac{\omega_g^2 A(\Omega)}{2A(\Omega) + R^q(\Omega)} \right] \tilde{y}_{2A/B}^q \\ &+ \left[\frac{2\omega_g^2}{R^+(\Omega)R^-(\Omega)} \frac{A(\Omega)R^q(\Omega)}{2A(\Omega) + R^q(\Omega)} \right] \tilde{y}_{2B/A}^q. \end{aligned} \quad (91)$$

B. apparent entanglement of outgoing light fields

As mentioned in the Introduction, probing gravity-induced entanglement (GIE) can offer strong evidence for quantum gravity [18–20, 26]. In our mutual-gravity optomechanical protocol, such entanglement could manifest in the outgoing light, as suggested by [19]. Paper I indicated that correlations in the outgoing light can also occur in the SN theory under the casual conditional framework, where mutual gravity is classical, and these correlations are nearly indistinguishable from those in quantum gravity. It remains unclear whether the complete entanglement structure is similarly indistinguishable.

Parameters	Symbol	Value
Mirror mass	M	10^{-3} kg
Mirror bare frequency	$\omega_m/(2\pi)$	0.5 Hz
SN frequency	$\omega_g/(2\pi)$	2×10^{-4} Hz
Quality factor	Q_m	3×10^7
Mechanical damping	$\gamma_m/(2\pi)$	1.67×10^{-8} Hz
Optical wavelength	λ	1064 nm
Cavity Finesse	\mathcal{F}	4000
Intra-cavity power	P_{cav}	2000 W

TABLE II. Sample parameters for the mutual-gravity optomechanical protocol.

Operationally, imagine that future experimentalists conduct such an optomechanical GIE experiment, obtain data from the projective measurement of the phases of the two outgoing fields, and subsequently process this data to compute an entanglement indicator such as the logarithmic negativity ε_N as defined in Eq.(23). Can a non-negative value of ε_N , extracted in this manner, serve as definitive evidence of quantum gravity? To address this question, it is necessary to perform a similar calculation for the mutual gravity protocol within the SN theory framework.

The Heisenberg-picture method offers a means to perform this calculation in the SN theory. Specifically, we need to compute the full covariance matrix of the outgoing light (24), focusing on the non-diagonal elements of matrices $\sigma_A = \sigma_B$ and σ_{AB} . Using Eq.(82), we have:

$$\begin{aligned} \tilde{y}_{1A/B}(\Omega) &= \tilde{y}_{1A/B}^q(\Omega), \\ \tilde{y}_{2A/B}(\Omega) &= \mathcal{T}_{AA/BB}(\Omega) \tilde{y}_{2A/B}^q(\Omega) + \mathcal{T}_{AB/BA}(\Omega) \tilde{y}_{2B/A}^q(\Omega), \end{aligned} \quad (92)$$

where

$$\begin{aligned} \mathcal{T}_{AA}(\Omega) &= \mathcal{T}_{BB}(\Omega) = 1 + \frac{\alpha \omega_g^4 K_{A/B}^{\pi/2 \text{Wiener}}(\Omega)}{R_+(\Omega)R_-(\Omega)}, \\ \mathcal{T}_{AB}(\Omega) &= \mathcal{T}_{BA}(\Omega) = \frac{\alpha \omega_g^2 R_q(\Omega) K_{B/A}^{\pi/2 \text{Wiener}}(\Omega)}{R_+(\Omega)R_-(\Omega)}. \end{aligned} \quad (93)$$

The covariance matrices σ_A and σ_{AB} are then:

$$\sigma_{A/B} = \begin{bmatrix} 1 & \mathcal{T}_{AA}^* \alpha^2 \chi_q^* \\ \mathcal{T}_{AA} \alpha^2 \chi_q & (|\mathcal{T}_{AA}|^2 + |\mathcal{T}_{AB}|^2)(1 + \alpha^4 |\chi_q|^2) \end{bmatrix}, \quad (94)$$

and

$$\sigma_{AB} = \sigma_{BA} \begin{bmatrix} 0 & \mathcal{T}_{AB}^* \alpha^2 \chi_q^* \\ \mathcal{T}_{AB} \alpha^2 \chi_q & 2\text{Re}[\mathcal{T}_{AA}^* \mathcal{T}_{BA}] (1 + \alpha^4 |\chi_q|^2) \end{bmatrix}. \quad (95)$$

Utilizing the sample parameters outlined in Table II, we plotted the logarithmic negativity as shown in Figure 6, comparing these findings to those derived from the quantum gravity framework. The results indicate that at zero temperature, both the SN theory and quantum gravity theory predict identical values for negativity. However, when accounting for the influence of a quantum thermal bath, this equivalence is quantitatively disrupted. Notably, the weak, apparent entanglement ($\epsilon_N > 0$) appears only under very low temperatures, as even a minor thermal effect can eliminate this apparent entanglement.

The influence of a quantum thermal bath on apparent entanglement is nuanced. In the SN theory, the expectation value of the displacement of mirrors A/B under the influence of a quantum bath remains zero, and thus, does not directly contribute to the classical gravity that impacts the motion of mirrors B/A. In contrast, within the framework of quantum gravity, the thermal bath can directly influence $\hat{x}_{A/B}$, subsequently affecting the evolution of the operator $\hat{x}_{B/A}$. Nevertheless, the thermal noise indirectly influences the mutual gravity protocol in SN theory by infiltrating the quantum trajectory of mirrors A/B through its additional contribution to the conditional variance $V_{xx}^{A/B}$. This differing impact of thermal noise on the dynamics of mutual gravity protocols in quantum gravity and SN theories accounts for the variations observed in negativity.

Finally, our analysis reveals that classical gravity can induce a apparent entanglement in the outgoing optical field within the SN theory. To correctly grasp the implications of this result for the GIE experiment, in particular for SN theory, it is beneficial to revisit the framework of the GIE experiment.

The conceptual foundation of the GIE experiment is based on the premise that quantum Newtonian mutual gravity can induce entanglement between two massive mirrors. However, experimentally accessing information about the mirror states can only be achieved through a detector interacting with the mirrors, which, in the context of the optomechanical protocol, is the optical field. Consequently, the entanglement between the mirrors is transferred to the optical field via optomechanical interactions, allowing it to manifest as entanglement in the optical domain.

Suppose some future experimentalists and theorists collaborated and designed such an experiment with the parameters listed in Tab. II. Then the experimentalist built and run the experimental apparatus, and collected the optical quadrature data of outgoing light A/B: $\tilde{y}_{\theta A/B}(t)$,

$$\tilde{y}_{\theta A/B}(t) = \sin \theta \tilde{y}_{1A/B}(t) + \cos \theta \tilde{y}_{2A/B}(t). \quad (96)$$

These data allow the experimentalist to *directly compute* their correlation function $C_{\tilde{y}_{\theta A/B} \tilde{y}_{\theta A/B}}(\tau)$, satisfying

$$\begin{aligned} C_{\tilde{y}_{\theta A/B} \tilde{y}_{\theta A/B}}(\tau) &= \sin^2 \theta C_{\tilde{y}_{1A/B} \tilde{y}_{1A/B}}(\tau) + \cos^2 \theta C_{\tilde{y}_{2A/B} \tilde{y}_{2A/B}}(\tau) \\ &\quad + \sin \theta \cos \theta C_{\tilde{y}_{1A/B} \tilde{y}_{2A/B}}(\tau). \end{aligned} \quad (97)$$

Measuring three different quadratures allows us to calculate $C_{\tilde{y}_{1A/B} \tilde{y}_{1A/B}}(\tau)$, $C_{\tilde{y}_{2A/B} \tilde{y}_{2A/B}}(\tau)$ and $C_{\tilde{y}_{1A/B} \tilde{y}_{2A/B}}(\tau)$, which the can be Fourier transformed to obtain the power spectrum (note that $S_{\tilde{y}_{1A/B} \tilde{y}_{1A/B}}(\Omega)$ and $S_{\tilde{y}_{2A/B} \tilde{y}_{2A/B}}(\Omega)$ are real, and the cross-spectrum can be complex) and thereby the covariance matrix.

However, the above prescription is valid only for quantum gravity, where everything is linear. The nonlinearity of the SN theory adds additional subtleties to this prescription. Note that the input-output relation in SN theory is given by Eq. (82) (or (92)), which can be formally written in the time domain as:

$$\begin{aligned} \tilde{y}_{\theta A/B}(t) &= \int_{-\infty}^t dt' \mathcal{T}_{AA/BB}^\theta(t-t')[\sin \theta, \cos \theta] \begin{bmatrix} \tilde{y}_{1A/B}^q(t') \\ \tilde{y}_{2A/B}^q(t') \end{bmatrix} \\ &\quad + \int_{-\infty}^t dt' \mathcal{T}_{AB/BA}^\theta(t-t')[\sin \theta, \cos \theta] \begin{bmatrix} \tilde{y}_{1B/A}^q(t') \\ \tilde{y}_{2B/A}^q(t') \end{bmatrix} \end{aligned} \quad (98)$$

Since the $\mathcal{T}_{AA/BB}^\theta(\Omega)$, $\mathcal{T}_{AB/BA}^\theta(\Omega)$ depend on θ , these relations become highly nonlinear. Therefore, we are not able to solve the cross-spectrum and the corresponding covariance matrix using the previous prescription. Moreover, if Nature followed SN theory while the experimentalists did not know and believed in QG, then the experimentalists analyzed their data using Eq. (96) rather than Eq. (98). Then, this prescription will lead to a θ -dependent negativity, which physically makes no sense. Finally, although the apparent entanglement can be calculated for SN theory, it remains an open question of finding a proper experimental state tomography method for the outgoing optical state.

VII. DISCUSSION AND CONCLUSION

In conclusion, this study introduces a Heisenberg-picture approach for analyzing the Schrödinger-Newton theory within the causal conditional framework, which incorporates the impact of continuous quantum measurement on system dynamics. We have demonstrated the equivalence between this Heisenberg-picture method and the Schrödinger-picture method previously employed in Paper I. Utilizing these theoretical tools, we further examined two optomechanical protocols aimed at testing the SN theory and probing gravity-induced entanglement (GIE) by analyzing the correlation matrix of the output optical fields. Our findings indicate that classical gravity can lead to apparent entanglement between the two output light fields, potentially serving as a false alarm in experiments designed to demonstrate the quantum nature of Newtonian gravity through optical field entanglement.

Significantly, the SN dynamics in the mutual gravity protocol can be interpreted as a *Local Operations and Classical Communications (LOCC)* [67, 68] interaction process. Building on the findings from Paper I, this study provides a concrete example of how LOCC-type interactions can imitate quantum interactions, potentially leading to false alarm of quantum effects. Intriguingly, recent work [16] by the Plenio group addresses this issue by developing a methodology to test the quantumness of gravity without relying on entanglement. In

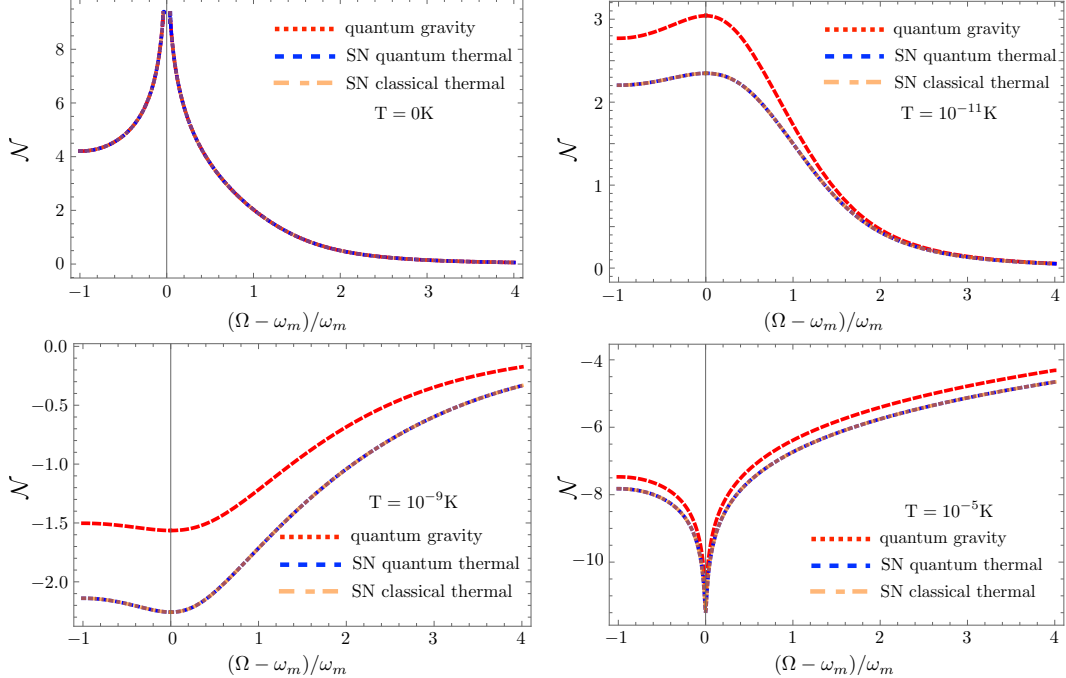


FIG. 6. Apparent entanglement of the outgoing optical fields in the mutual gravity protocol, where \mathcal{N} is defined from the logarithmic negativity $\epsilon_N = \max\{\mathcal{N}, 0\}$ and $\mathcal{N} = -(1/2)\ln\left[\left(\Sigma - \sqrt{\Sigma^2 - 4\det\sigma}\right)/2\right]$ where $\mathcal{N} > 0$ means the exist of entanglement. The blue-dashed curve is the \mathcal{N} of the outgoing optical state in the SN theory at different frequencies, where the thermal noise is treated quantum mechanically. For comparison, the orange and red curves are the \mathcal{N} in the SN theory when the thermal noise is treated classically and in the quantum gravity theory, respectively. The details of the influence of classical thermal noise are discussed in Appendix C

their research, they quantify the maximum fidelity with which any classical interaction, such as a LOCC-type interaction, can replicate a given quantum interaction. It is important to note that the fidelity between the conditional mirror states prepared under continuous measurement in both quantum gravity and SN theory is expected to adhere to Plenio's upper bound, a topic that will be explored in future work.

Furthermore, several points need to be discussed to provide some insights into understanding this apparent entanglement.

Unentangled mirrors—In quantum gravity, the entanglement of the two optical fields can be attributed back to the entanglement of the two mirror oscillators, induced by the quantum Newtonian mutual gravity [19]. In contrast, there is *no entanglement* between the mirror oscillators since the classical Newtonian gravity can not transfer quantum information [1]. The “apparent entanglement” of the two outgoing light fields exists only because the SN dynamics of mirror B depend on the measurement outcome of mirror A in the causal conditional formalism, which is a feature of the SN theory as a nonlinear quantum mechanics. However, as we have shown in Fig. 5, this apparent entanglement is sufficient to be a false alarm for quantum gravity.

Quantum state—Heisenberg picture analysis of the self-gravity and mutual gravity optomechanical protocol reveals interesting features of the light field interacting with the test mass state in the Schrödinger-Newton theory. In particular,

for the mutual-gravity case, we obtained a apparent entanglement in the SN theory which is almost indistinguishable from the real entanglement if the gravity is quantum. Entanglement measures the non-separable feature of the quantum state, therefore the quantum state of the optical fields here deserves a further discussion.

In standard quantum mechanics (or when the gravity is quantum), the quantum state (or the wavefunction) is considered to be the physical reality according to the standard interpretation. In a unitary process, the quantum state evolves linearly; while in a quantum measurement process, the quantum state manifests its statistical characters. However, experimentally extracting the quantum information in the quantum state generally requires a quantum measurement process that collapses the quantum state. The experimentalists collect the data from the measurement ensemble, reconstruct the data statistics, and finally reconstruct the quantum state. This process is called *quantum tomography*. In standard quantum mechanics, suppose we have a state $|\psi(t)\rangle$ evolved unitarily from an initial state $|\psi(0)\rangle$. The state obtained by quantum tomography on the $|\psi(t)\rangle$ is the same as $|\psi(t)\rangle$ in standard quantum mechanics.

In the SN theory, subtleties arise due to its inherent non-linearity. For an initially unentangled joint optical state given by $|\psi_{\text{opt}}(0)\rangle = |0\rangle_A \otimes |0\rangle_B$, the evolution of the state will depend on the measurement outcomes $\tilde{y}_{\theta A}, \tilde{y}_{\theta B}$. This depen-

dence occurs because these measurement outcomes determine the conditional mechanical state, which in turn modulates the incoming optical field. Consequently, the evolution operator for the optical state $|\psi_{\text{opt}}(t)\rangle$ incorporates $\tilde{y}_{\theta A/B}$. Intriguingly, if the standard approach is employed to reconstruct the optical quantum state from the covariance matrix—akin to quantum state tomography—the entanglement attribute will manifest as positive negativity, provided thermal effects are sufficiently minimized. Conversely, a direct derivation of the causal conditional dynamics from first principles reveals that such perceived entanglement is only apparent, and no actual entanglement exists in the state $|\psi_{\text{opt}}(t)\rangle$. This discrepancy highlights a break in the equivalency that holds in standard quantum mechanics, signaling a subtle complexity in interpreting the wave function within the SN framework.

Regarding the experiment designed to probe quantum gravity such as GIE-experiment, the potential false alarm found in this work shows that carefully designing the experiment for circumventing the effect of quantum trajectory induced by continuous quantum measurement is important, which we will leave for future work.

ACKNOWLEDGMENTS

Y.M. thanks Professor Chunnong Zhao for the useful discussions. Y.M. is supported by the National Key R&D Program of China “Gravitational Wave Detection” (Grant No. 2023YFC2205801), National Natural Science Foundation of China under Grant No.12474481, and the start-up funding provided by Huazhong University of Science and Technology. Y. C. is supported by the Simons Foundation (Award Number 569762).

Appendix A: Equivalence of Wiener filter method and the stochastic master equation method in standard quantum mechanics

In this section, we discuss two methods that can obtain the conditional expectation value in standard quantum mechanics, using an exemplary optomechanical system. Firstly, we present the Wiener method and its application in the optomechanism system. Secondly, we present the stochastic master equation method and calculate the Kalman filter to obtain the steady-state conditional expectation value. Lastly, we prove that these methods are exactly equivalent in the steady state of a continuous measurement process.

1. The Wiener filter method

A simple optomechanical system has the following equations of motion:

$$\begin{aligned} M\ddot{\hat{x}} &= -M\omega_m^2\hat{x} - \gamma M\dot{\hat{x}} + \alpha\hat{a}_1 \\ \hat{b}_\theta &= \cos\theta\hat{a}_1 + \sin\theta\hat{a}_2 + \sin\theta\alpha\hat{x} \end{aligned} \quad (\text{A1})$$

The minimum means square estimator (MMSE) on the measurement record (on the \hat{b}_θ) database \tilde{y}_θ gives the conditional expectation of mechanical displacement $\langle x(t) \rangle_c$ as follows. The estimator of the mechanical displacement can be constructed with the filter function $K(t - t')$,

$$x_{\text{est}}(t) = \int_{-\infty}^t K(t - t')\tilde{y}_\theta(t')dt', \quad (\text{A2})$$

where the MMSE requests that the filter function $K(t - t')$ satisfies the variational principle:

$$\frac{\delta}{\delta K} \left\langle \left(\hat{x}(t) - \int_{-\infty}^t K(t - t')\tilde{y}_\theta(t')dt' \right)^2 \right\rangle = 0. \quad (\text{A3})$$

This variational principle leads to an integral equation that must be satisfied by the filter called the Wiener filter $K_w(t - t')$:

$$C_{x\tilde{y}_\theta}(t - t'') = \int_{-\infty}^t dt' K_w(t - t') C_{\tilde{y}_\theta\tilde{y}_\theta}(t' - t''), \quad t'' \leq t, \quad (\text{A4})$$

where C_{AB} is the correlation function of quantities A, B . This result can also be understood as the error of the estimator $\hat{x}(t) - x_{\text{est}}(t)$ have no correlation with the past measurement data $\tilde{y}_\theta(t' < t)$. The Wiener filter can be computed by the Wiener-Hopf equation in the frequency domain.

This integral equation can be solved via the Wiener-Hopf method:

$$K_{\text{Wiener}}(\Omega) = \frac{1}{\phi_+(\Omega)} \left[\frac{S_{x\tilde{y}_\theta}(\Omega)}{\phi_-(\Omega)} \right]_+ \quad (\text{A5})$$

In the above formula, we decompose the outgoing spectrum as $S_{\tilde{y}_\theta\tilde{y}_\theta}(\Omega) = \phi_+(\Omega)\phi_-(\Omega)$, where the $\phi_\pm(\Omega)$ and their inverse are analytical in the upper/lower-half complex Ω -plane. The $[...]_+$ also means that we only take the part which is analytical in the upper complex Ω -plane. In order to obtain the Wiener-filtering function, we need to have $\phi_\pm(\Omega)$ and $S_{x\tilde{y}_\theta}(\Omega)$.

First, it is straightforward to show that

$$S_{\tilde{y}_\theta\tilde{y}_\theta} = \frac{\sin^2\theta\alpha^4 + M\alpha^2\sin 2\theta(\omega_m^2 - \Omega^2)}{M^2|\omega_m^2 - \Omega^2 - i\gamma_m\Omega|^2} + 1, \quad (\text{A6})$$

which can be rearranged as

$$S_{\tilde{y}_\theta\tilde{y}_\theta} = \frac{(\Omega - \beta)(\Omega + \beta)(\Omega - \beta_c)(\Omega + \beta_c)}{(\Omega - \eta)(\Omega + \eta)(\Omega - \eta_c)(\Omega + \eta_c)}, \quad (\text{A7})$$

where

$$\begin{aligned} \beta &= a + ib, \quad \beta_c = a - ib, \\ \eta &= \frac{\sqrt{-\gamma_m^2 + 4\omega_m^2}}{2} - i\frac{\gamma_m}{2}, \end{aligned} \quad (\text{A8})$$

with

$$a = \frac{\sqrt{a_1 + \sqrt{a_2}}}{2}, \quad b = -\frac{\sqrt{-a_1^2 - a_2}}{4a}, \quad (\text{A9})$$

and

$$\begin{aligned} a_1 &= -\gamma_m^2 + 2\omega_m^2 + \Lambda^2 \sin 2\theta, \\ a_2 &= 2\Lambda^4(1 - \cos 2\theta) + 4\omega_m^2(\omega_m^2 + \Lambda^2 \sin 2\theta). \end{aligned} \quad (\text{A10})$$

Then according to the definition of $\phi_{\pm}(\Omega)$, we have:

$$\begin{aligned} \phi_+(\Omega) &= \frac{(\Omega - \beta)(\Omega + \beta_c)}{(\Omega - \eta)(\Omega + \eta_c)}, \\ \phi_-(\Omega) &= \frac{(\Omega - \beta_c)(\Omega + \beta)}{(\Omega - \eta_c)(\Omega + \eta)}. \end{aligned} \quad (\text{A11})$$

Secondly, we have

$$\begin{aligned} S_{x\bar{y}_\theta} &= \cos \theta \alpha S_{xy_1} + \sin \theta \alpha S_{xx} \\ &= \frac{\sin \theta \alpha^3 - \cos \theta \alpha M(\Omega + \eta)(\Omega - \eta_c)}{M^2(\Omega - \eta)(\Omega + \eta)(\Omega - \eta_c)(\Omega + \eta_c)}. \end{aligned} \quad (\text{A12})$$

This $S_{x\bar{y}_\theta}$, together with Eq.(A11) and some tedious alegbras, leads to,

$$\left[\frac{S_{xb_2}}{\phi_-} \right]_+ = \frac{\beta \beta_c + \Omega(\beta - \beta_c) + i\gamma_m \Omega - \omega_m^2}{\alpha \sin \theta ((\eta - \Omega)(\Omega + \eta_c))}. \quad (\text{A13})$$

Therefore, by the definition Eq. (A5), it is straightforward to obtain the Wiener filter function:

$$K_{\text{Wiener}}(\Omega) = \frac{\beta \beta_c + \Omega(\beta - \beta_c) + i\gamma_m \Omega - \omega_m^2}{\alpha \sin \theta (\beta - \Omega)(\Omega + \beta_c)}. \quad (\text{A14})$$

2. The filter derived from the stochastic master equation and the equivalency

The method and the formal solution is exactly the same as in the main text. The obtained Kalman filter function at the long-time tail can be written as:

$$K_{\text{Kalman}}(\Omega) = \frac{A_m(\Omega)}{\alpha \sin \theta (A_m(\Omega) - R_m(\Omega))}. \quad (\text{A15})$$

Where,

$$\begin{aligned} A_m(\Omega) &= V_{xx} \alpha^2 (V_{xx} \alpha^2 \cos 2\theta - V_{xx} \alpha^2 - 2\gamma_m + 2i\Omega) \sin^2 \theta \\ &\quad - \alpha^2 \sin \theta \cos \theta / M, \\ R_m(\Omega) &= \omega_m^2 - \Omega^2 - i\gamma_m \Omega. \end{aligned} \quad (\text{A16})$$

The only difference is the second order moment V_{xx} here takes the following form:

$$\begin{aligned} V_{xx} &= \frac{-\gamma_m}{2\alpha^2 \sin^2 \theta} + \\ &\quad \frac{\sqrt{\gamma_m^2 - 2\omega_m^2 - \Lambda^2 \sin 2\theta + 2\sqrt{\omega_m^4 + \Lambda^4 \sin^2 \theta + \Lambda^2 \omega_m^2 \sin 2\theta}}}{2\alpha^2 \sin^2 \theta}, \end{aligned} \quad (\text{A17})$$

which is obtained from the Riccati equation for an optomechanical continuous measurement in the standard quantum mechanics. This V_{xx} has a more compact form if we use the definition of β, β_c :

$$V_{xx} = \frac{-\gamma_m}{2\alpha^2 \sin^2 \theta} + \frac{i(\beta - \beta_c)}{2\alpha^2 \sin^2 \theta}. \quad (\text{A18})$$

Then the filter based on the master equation can be rearranged as:

$$\begin{aligned} K_{\text{Kalman}}(\Omega) &= \frac{1}{\alpha \sin \theta} \times \\ &\quad \frac{(\beta - \beta_c + i\gamma_m)(\beta - \beta_c - i\gamma_m - 2\Omega) - \alpha^2 \sin 2\theta / M}{(\beta - \Omega)^2 + (\beta_c + \Omega)^2 - 2\beta \beta_c + \gamma_m^2 - 2\omega_m^2 - \alpha^2 \sin 2\theta / M}. \end{aligned} \quad (\text{A19})$$

Using the definition of β and β_c , we can derive the following useful relation:

$$\begin{aligned} \omega_m &= \sqrt{\frac{\beta^2 + \beta_c^2 + \gamma_m^2 - \Lambda^2 \sin 2\theta}{2}}, \\ \Lambda &= \sqrt{\frac{\beta^2 + \beta_c^2 + \gamma_m^2 - 2\omega_m^2}{\sin 2\theta}}. \end{aligned} \quad (\text{A20})$$

Combining Eq. A19 and Eq. A20 leads to,

$$K_{\text{Kalman}}(\Omega) = \frac{\beta \beta_c + \Omega(\beta - \beta_c) + i\gamma_m \Omega - \omega_m^2}{\alpha \sin \theta (\beta - \Omega)(\Omega + \beta_c)}, \quad (\text{A21})$$

which is exactly equal to Eq.(A14). Therefore, for optomechanical continuous measurement in standard quantum mechanics, the Wiener filter method and the master equation method are exactly equivalent.

Appendix B: Prove the equality satisfied by the spectrum $S_{\bar{y}_\theta \bar{y}_\theta^q}$ in SN theory.

Here we present the proof of an equality that is used in the main text to simplify the formula.

Direct calculation of the $S_{\bar{y}_\theta \bar{y}_\theta^q}$ from the input-output relation b_θ^q leads to:

$$S_{\bar{y}_\theta \bar{y}_\theta^q} = \frac{M^2 |R_q(\Omega)|^2 + \alpha^4 \sin^2 \theta + M \alpha^2 \sin 2\theta (\omega_q^2 - \Omega^2)}{M^2 |R_q(\Omega)|^2}. \quad (\text{B1})$$

Using Eq.A16-18, and replace the ω_m in Eq.A17 by ω_q , we obtain,

$$A_q^\theta(\Omega) = \frac{M(\beta - \beta_c + i\gamma_m)(\beta - \beta_c - i\gamma_m - 2\Omega) - \alpha^2 \sin(2\theta)}{2M}. \quad (\text{B2})$$

On the other hand, using Eq. B2 and $R_q(\Omega) = \omega_q^2 - \Omega^2 - i\gamma_m \Omega$, we have,

$$\begin{aligned} |A_q^\theta(\Omega) - R_q(\Omega)|^2 = & |R_q(\Omega)|^2 - \frac{(\beta - \beta_c)^2(\beta + \beta_c)^2}{4} \\ & + \frac{\gamma_m^2(\gamma_m^2 - 4\omega_q^2)}{4} - \frac{\alpha^2\gamma_m^2 \sin(2\theta)}{2M} \\ & + \frac{\alpha^2(\omega_q^2 - \Omega^2)\sin(2\theta)}{M} + \frac{\alpha^4 \sin^2(2\theta)}{4M^2}. \end{aligned} \quad (\text{B3})$$

During the above derivation, the following relation has been used:

$$\beta^2 + \beta_c^2 = -\gamma_m^2 + 2\omega_q^2 + \frac{\alpha^2}{M} \sin(2\theta). \quad (\text{B4})$$

Using the definition of β and β_c , we have:

$$\begin{aligned} (\beta - \beta_c)^2(\beta + \beta_c)^2 = & \gamma_m^4 - 4\gamma_m^2\omega_q^2 - 2\frac{\alpha^2\gamma_m^2 \sin(2\theta)}{M} \\ & - 4\frac{\alpha^4 \sin^4(\theta)}{M^2}. \end{aligned} \quad (\text{B5})$$

Substituting Eq. B5 into Eq. B3, we obtain

$$\begin{aligned} |A_q^\theta(\Omega) - R_q(\Omega)|^2 = & |R_q(\Omega)|^2 + \frac{\alpha^4 \sin^2 \theta}{M^2} \\ & + \frac{\alpha^2(\omega_q^2 - \Omega^2)\sin(2\theta)}{M}. \end{aligned} \quad (\text{B6})$$

Combining Eq. B6 and Eq. B1, we obtain:

$$S_{\tilde{y}_\theta \tilde{y}_\theta} = \frac{|A_q^\theta(\Omega) - R_q(\Omega)|^2}{|R_q(\Omega)|^2}. \quad (\text{B7})$$

Appendix C: The effect of classical thermal noise

Nonlinear quantum mechanics theory such as Schrödinger-Newton theory has a subtle issue when dealing with environmental thermal noise, which was detailed in [22]. In the main text, we have focused on the prescription of thermal noise completely attributed to the quantum origin. In this section, we follow a different prescription for thermal noise proposed in [22], where the thermal noise is separated into the classical and the quantum part.

$$\hat{F}_{\text{th}}(t) = f_{\text{cl}}(t) + \hat{f}_{\text{zp}}(t), \quad (\text{C1})$$

where

$$f_{\text{cl}}(t) = \langle \hat{F}_{\text{th}}(t) \rangle, \quad \hat{f}_{\text{zp}}(t) = \hat{F}_{\text{th}}(t) - \langle \hat{F}_{\text{th}}(t) \rangle. \quad (\text{C2})$$

The total thermal noise spectrum is represented by:

$$S_{F_{\text{th}} F_{\text{th}}}(\Omega) = 4\hbar \left[\frac{1}{e^{\frac{\hbar\Omega}{k_B T}} - 1} + \frac{1}{2} \right] \frac{\text{Im}[\chi_m(\Omega)]}{|\chi_m(\Omega)|^2}. \quad (\text{C3})$$

Using the approach of the paper [22], the total thermal noise spectrum is separated into the quantum part and classical part as follows,

$$\begin{aligned} S_{f_{\text{cl}} f_{\text{cl}}}(\Omega) &= 4\hbar \frac{1}{e^{\frac{\hbar\Omega}{k_B T}} - 1} \frac{\text{Im}[\chi_m(\Omega)]}{|\chi_m(\Omega)|^2} \approx 4k_B T M \gamma_m, \\ S_{f_{\text{zp}} f_{\text{zp}}}(\Omega) &= 2\hbar \frac{\text{Im}[\chi_m(\Omega)]}{|\chi_m(\Omega)|^2} \approx 2\hbar \Omega M \gamma_m. \end{aligned} \quad (\text{C4})$$

In the high-temperature limit, we assume the thermal noise is dominantly classical $S_{f_{\text{cl}} f_{\text{cl}}}(\Omega) \gg S_{f_{\text{zp}} f_{\text{zp}}}(\Omega)$.

Now, we discuss the effect of classical thermal noise on the self-gravity protocol as an example. In the Heisenberg picture, the classical thermal noise modifies the evolution equation as,

$$\begin{aligned} \dot{\hat{x}} &= \frac{\hat{p}}{M}, \\ \dot{\hat{p}} &= -M\omega_m^2 \hat{x} - M\omega_{SN}^2(\hat{x} - \langle \hat{x} \rangle) + \hbar\alpha\hat{a}_1 + f_{\text{cl}}, \\ \hat{b}_1 &= \hat{a}_1, \\ \hat{b}_\theta &= \cos\theta\hat{a}_2 + \sin\theta\hat{a}_1 + \sin\theta\alpha\hat{x}, \end{aligned} \quad (\text{C5})$$

where the outgoing field can be solved as:

$$\begin{aligned} \hat{b}_\theta(t) &= \cos\theta\hat{a}_1 + \sin\theta\hat{a}_2 \\ &+ \sin\theta\alpha \int_{-\infty}^t \chi_q(t-t')(\hbar\alpha\hat{a}_1(t') + M\omega_{SN}^2\langle \hat{x}(t') \rangle + f_{\text{cl}}(t'))dt'. \end{aligned} \quad (\text{C6})$$

Similarly, the thermal noise affect the displacement of mirror \hat{x} in its classical part x_{cl} while preserving its quantum part \hat{x}_q ,

$$\begin{aligned} \hat{x}_q(t) &= \int_{-\infty}^t \chi_q(t-t')\hbar\alpha\hat{a}_1(t')dt', \\ x_{\text{cl}}(t) &= \int_{-\infty}^t \chi_q(t-t')(M\omega_{SN}^2\langle \hat{x}(t') \rangle + f_{\text{cl}}(t'))dt'. \end{aligned} \quad (\text{C7})$$

Since the quantum part is unaffected, the Wiener filter that is used to estimate $\langle \hat{x}_q \rangle$ is unchanged, and thus we have:

$$\langle \hat{x}_q \rangle(t) = \int_{-\infty}^t K_q(t-t')\tilde{y}_\theta^q. \quad (\text{C8})$$

Transforming into the frequency domain:

$$\langle \hat{x}(\Omega) \rangle = \frac{\chi_m(\Omega)}{\chi_q(\Omega)} K_q(\Omega) \tilde{y}_\theta^q(\Omega) + \chi_m(\Omega) f_{\text{cl}}(\Omega). \quad (\text{C9})$$

Now we can derive the formula for the output data taking into account the classical noise:

$$\tilde{y}_\theta(\Omega) = \tilde{y}_\theta^q(\Omega) + \chi_q(\Omega)[\sin\theta\alpha M\omega_{SN}^2\langle \hat{x}(\Omega) \rangle + \sin\theta\alpha f_{\text{cl}}(\Omega)]. \quad (\text{C10})$$

Using the Wiener filter function,

$$K_q(\Omega) = \frac{A_q^\theta(\Omega)}{\alpha \sin\theta(A_q^\theta(\Omega) - R_q(\Omega))}, \quad (\text{C11})$$

the outgoing result can be derived as:

$$\tilde{y}_\theta(\Omega) = \left[\frac{R_q(\Omega)}{R_m(\Omega)} \frac{A_q^\theta(\Omega) - R_m(\Omega)}{A_q^\theta(\Omega) - R_q(\Omega)} \right] \tilde{y}_\theta^0(\Omega) + \alpha \sin \theta \chi_m(\Omega) f_{\text{cl}}(\Omega), \quad (\text{C12})$$

therefore, the noise spectrum of the outgoing field becomes:

$$S_{\tilde{y}_\theta \tilde{y}_\theta} = \frac{|A_q^\theta(\Omega) - R_m(\Omega)|^2}{|R_m(\Omega)|^2} + \sin^2 \theta \alpha^2 |\chi_m(\Omega)|^2 S_{f_{\text{cl}} f_{\text{cl}}}(\Omega). \quad (\text{C13})$$

Using the expression of $A_q^\theta(\Omega)$ and $R_m(\Omega)$, the noise spectrum can be represented by:

$$\begin{aligned} S_{\tilde{y}_\theta \tilde{y}_\theta}(\Omega) = & 1 + |\chi_m(\Omega)|^2 [\alpha^4 \sin^4 \theta + \alpha^2 \sin 2\theta (\omega_m^2 - \Omega^2)] \\ & + 4|\chi_m(\Omega)|^2 \sin \theta^2 \alpha^2 M \gamma_m k_B T + \omega_{\text{SN}}^2 M^2 |\chi_m(\Omega)|^2 \times \\ & \left(2\omega_q^2 + \Lambda^2 \sin 2\theta - 2\sqrt{(\Lambda^4 \sin^2 \theta + \omega_q^2 + 2\Lambda^2 \omega_q^2 \sin 2\theta)} \right). \end{aligned} \quad (\text{C14})$$

The influence of the classical thermal noise on the mutual gravity protocol can be similarly analyzed.

In the main text, Fig. 4 and Fig. 6 depict the effects of classical thermal noise in both SN self-gravity and mutual SN gravity cases. These results indicate that the influence of classical thermal noise closely resembles that observed in quantum gravity scenarios. Specifically, in the self-gravity case, this similarity arises because classical thermal force noise, which is a c-number f_{cl} drives the classical component of \hat{x} in the same way as the quantum thermal noise operator \hat{f}_{th} drives

the quantum displacement operator \hat{x} in the quantum gravity scenario. Concretely speaking, we have:

$$\begin{aligned} \hat{x}(\Omega) &= \hat{x}_q(\Omega) + x_{\text{cl}}(\Omega), \\ x_{\text{cl}}(\Omega) &= M \omega_{\text{SN}}^2 \chi_m(\Omega) K_q(\Omega) \tilde{y}_\theta^0(\Omega) + \chi_m(\Omega) f_{\text{cl}}(\Omega), \end{aligned} \quad (\text{C15})$$

where \hat{x}_q is unaffected by classical thermal noise. For comparison, in the case of quantum gravity, the displacement operator of the mirror satisfies:

$$\hat{x}(\Omega) = \chi_m(\Omega) \hbar \alpha \hat{a}_1(\Omega) + \chi_m(\Omega) \hat{f}_{\text{th}}(\Omega). \quad (\text{C16})$$

These two equations demonstrate that the influence of thermal noise manifests in a highly similar manner. Similarly, in the mutual SN gravity scenario, under the causal conditional framework, the classical thermal noise *randomly* and *directly* drives the conditional mean of one mirror by influencing the classical component of its \hat{x} . The thermal-driven classical stochastic motion of the mirror generates a stochastic gravitational field, which subsequently exerts a random force on the second mirror. Therefore, the optical field reflected from the second mirror motion contains information about the thermal driving of the first mirror. Similar to the self-gravity case, in the mutual SN gravity scenario, the mirror's response to classical thermal noise exhibits a form similar to that observed in the quantum gravity case [19], except the \hat{f}_{th} is replaced by f_{cl} . However, in the case of a large thermal occupation number, the f_{cl} and \hat{F}_{th} follow almost identical statistical distributions. Therefore, if the thermal noise is treated classically, the differences in the correlation spectrum between SN gravity and quantum gravity cases become negligible, as shown in Fig. 6.

* yanbei@caltech.edu

† myqphy@hust.edu.cn

- [1] Yubao Liu, Haixing Miao, Yanbei Chen, and Yiqiu Ma. Semi-classical gravity phenomenology under the causal-conditional quantum measurement prescription. *Phys. Rev. D*, 107:024004, Jan 2023.
- [2] Markus Aspelmeyer, Tobias J. Kippenberg, and Florian Marquardt. Cavity optomechanics. *Reviews of Modern Physics*, 86(4):1391–1452, October 2014.
- [3] Yanbei Chen. Macroscopic quantum mechanics: theory and experimental concepts of optomechanics. *Journal of Physics B: Atomic, Molecular and Optical Physics*, 46(10):104001, may 2013.
- [4] Markus Aspelmeyer. Quantum optomechanics: exploring the interface between quantum physics and gravity. In *APS Division of Atomic, Molecular and Optical Physics Meeting Abstracts*, volume 43 of *APS Meeting Abstracts*, page C6.004, June 2012.
- [5] Thai M. Hoang, Yue Ma, Jonghoon Ahn, Jaehoon Bang, F. Robicheaux, Zhang-Qi Yin, and Tongcang Li. Torsional optomechanics of a levitated nonspherical nanoparticle. *Phys. Rev. Lett.*, 117:123604, Sep 2016.
- [6] David Mason, Junxin Chen, Massimiliano Rossi, Yeghishe Tsaturyan, and Albert Schliesser. Continuous force and displacement measurement below the standard quantum limit. *Nature Physics*, 15(8):745–749, 2019.

- [7] Massimiliano Rossi, David Mason, Junxin Chen, Yeghishe Tsaturyan, and Albert Schliesser. Measurement-based quantum control of mechanical motion. *Nature*, 563(7729):53–58, 2018.
- [8] A M Jayich, J C Sankey, B M Zwickl, C Yang, J D Thompson, S M Girvin, A A Clerk, F Marquardt, and J G E Harris. Dispersive optomechanics: a membrane inside a cavity. *New Journal of Physics*, 10(9):095008, sep 2008.
- [9] Haocun Yu, L. McCuller, M. Tse, N. Kijbunchoo, L. Barsotti, N. Mavalvala, and members of the LIGO Scientific Collaboration. Quantum correlations between light and the kilogram-mass mirrors of ligo. *Nature*, 583(7814):43–47, 2020.
- [10] Nancy Aggarwal, Torrey J. Cullen, Jonathan Cripe, Garrett D. Cole, Robert Lanza, Adam Libson, David Follman, Paula Heu, Thomas Corbitt, and Nergis Mavalvala. Room-temperature optomechanical squeezing. *Nature Physics*, 16(7):784–788, 2020.
- [11] Seth B. Cataño Lopez, Jordy G. Santiago-Condori, Keiichi Edamatsu, and Nobuyuki Matsumoto. High- q milligram-scale monolithic pendulum for quantum-limited gravity measurements. *Phys. Rev. Lett.*, 124:221102, Jun 2020.
- [12] Masaki Ando, Koji Ishidoshiro, Kazuhiro Yamamoto, Kent Yagi, Wataru Kokuyama, Kimio Tsubono, and Akiteru Takamori. Torsion-bar antenna for low-frequency gravitational-wave observations. *Phys. Rev. Lett.*, 105:161101, Oct 2010.
- [13] Amit Singh Ubhi, Leonid Prokhorov, Sam Cooper, Chiara Di

- Fronzo, John Bryant, David Hoyland, Alexandra Mitchell, Jesse Van Dongen, Conor Mow-Lowry, Alan Cumming, et al. Active platform stabilization with a 6d seismometer. *Applied Physics Letters*, 121(17), 2022.
- [14] David Edward Bruschi Richard Howl, Lucia Hackermüller and Ivette Fuentes. Gravity in the quantum lab. *Advances in Physics: X*, 3(1):1383184, 2018.
- [15] Daniel Carney, Philip C E Stamp, and Jacob M Taylor. Tabletop experiments for quantum gravity: a user’s manual. *Classical and Quantum Gravity*, 36(3):034001, jan 2019.
- [16] Ludovico Lami, Julen S. Pedernales, and Martin B. Plenio. Testing the quantumness of gravity without entanglement. *Phys. Rev. X*, 14:021022, May 2024.
- [17] Alessio Belenchia, Robert M. Wald, Flaminia Giacomini, Esteban Castro-Ruiz, Časlav Brukner, and Markus Aspelmeyer. Quantum superposition of massive objects and the quantization of gravity. *Phys. Rev. D*, 98:126009, Dec 2018.
- [18] Sougato Bose, Anupam Mazumdar, Gavin W. Morley, Hendrik Ulbricht, Marko Toroš, Mauro Paternostro, Andrew A. Geraci, Peter F. Barker, M. S. Kim, and Gerard Milburn. Spin entanglement witness for quantum gravity. *Phys. Rev. Lett.*, 119:240401, Dec 2017.
- [19] Haixing Miao, Denis Martynov, Huan Yang, and Animesh Datta. Quantum correlations of light mediated by gravity. *Phys. Rev. A*, 101:063804, Jun 2020.
- [20] Tanjung Krisnanda, Guo Yao Tham, Mauro Paternostro, and Tomasz Paterek. Observable quantum entanglement due to gravity. *npj Quantum Information*, 6(1):12, 2020.
- [21] Huan Yang, Haixing Miao, Da-Shin Lee, Bassam Helou, and Yanbei Chen. Macroscopic quantum mechanics in a classical spacetime. *Phys. Rev. Lett.*, 110:170401, Apr 2013.
- [22] Bassam Helou, Jun Luo, Hsien-Chi Yeh, Cheng-gang Shao, B. J. J. Slagmolen, David E. McClelland, and Yanbei Chen. Measurable signatures of quantum mechanics in a classical spacetime. *Phys. Rev. D*, 96:044008, Aug 2017.
- [23] André Großardt, James Bateman, Hendrik Ulbricht, and Angelo Bassi. Optomechanical test of the schrödinger-newton equation. *Phys. Rev. D*, 93:096003, May 2016.
- [24] C. C. Gan, C. M. Savage, and S. Z. Scully. Optomechanical tests of a schrödinger-newton equation for gravitational quantum mechanics. *Phys. Rev. D*, 93:124049, Jun 2016.
- [25] Animesh Datta and Haixing Miao. Signatures of the quantum nature of gravity in the differential motion of two masses. *Quantum Science and Technology*, 6(4):045014, aug 2021.
- [26] Ryan J. Marshman, Anupam Mazumdar, and Sougato Bose. Locality and entanglement in table-top testing of the quantum nature of linearized gravity. *Phys. Rev. A*, 101:052110, May 2020.
- [27] Daine L. Danielson, Gautam Satishchandran, and Robert M. Wald. Gravitationally mediated entanglement: Newtonian field versus gravitons. *Phys. Rev. D*, 105:086001, Apr 2022.
- [28] Marios Christodoulou, Andrea Di Biagio, Markus Aspelmeyer, Časlav Brukner, Carlo Rovelli, and Richard Howl. Locally mediated entanglement in linearized quantum gravity. *Phys. Rev. Lett.*, 130:100202, Mar 2023.
- [29] Stefan Nimmrichter and Klaus Hornberger. Stochastic extensions of the regularized schrödinger-newton equation. *Phys. Rev. D*, 91:024016, Jan 2015.
- [30] Mueller C. *Les Théories Relativistes de la Gravitation (Colloques Internationaux CNRS)*, edited by A Lichnerowicz and M-A Tonnelat. Paris: CNRS, 1962.
- [31] L. Rosenfeld. On quantization of fields. *Nuclear Physics*, 40:353–356, February 1963.
- [32] L. Diósi. Models for universal reduction of macroscopic quantum fluctuations. *Phys. Rev. A*, 40:1165–1174, Aug 1989.
- [33] Roger Penrose. On gravity’s role in quantum state reduction. *General Relativity and Gravitation*, 28(5):581–600, 1996.
- [34] Lajos Diósi and Jonathan J. Halliwell. Coupling classical and quantum variables using continuous quantum measurement theory. *Phys. Rev. Lett.*, 81:2846–2849, Oct 1998.
- [35] S Carlip. Is quantum gravity necessary? *Classical and Quantum Gravity*, 25(15):154010, jul 2008.
- [36] Mohammad Bahrami, André Großardt, Sandro Donadi, and Angelo Bassi. The schrödinger–newton equation and its foundations. *New Journal of Physics*, 16(11):115007, nov 2014.
- [37] Angelo Bassi, André Großardt, and Hendrik Ulbricht. Gravitational decoherence. *Classical and Quantum Gravity*, 34(19):193002, sep 2017.
- [38] Jonathan Oppenheim, Carlo Sparaciari, Barbara Šoda, and Zachary Weller-Davies. Gravitationally induced decoherence vs space-time diffusion: testing the quantum nature of gravity. *Nature Communications*, 14(1):7910, 2023.
- [39] Jonathan Oppenheim. A postquantum theory of classical gravity? *Phys. Rev. X*, 13:041040, Dec 2023.
- [40] Don N. Page and C. D. Geilker. Indirect evidence for quantum gravity. *Phys. Rev. Lett.*, 47:979–982, Oct 1981.
- [41] Sougato Bose, Ivette Fuentes, Andrew A Geraci, Saba Mehsar Khan, Sofia Qvarfort, Markus Rademacher, Muddassar Rashid, Hendrik Ulbricht, and Clara C Wanjura. Massive quantum systems as interfaces of quantum mechanics and gravity. *arXiv preprint arXiv:2311.09218*, 2023.
- [42] D Kafri, G J Milburn, and J M Taylor. Bounds on quantum communication via newtonian gravity. *New Journal of Physics*, 17(1):015006, jan 2015.
- [43] Daniel Carney, Holger Müller, and Jacob M. Taylor. Using an atom interferometer to infer gravitational entanglement generation. *PRX Quantum*, 2:030330, Aug 2021.
- [44] D Kafri, J M Taylor, and G J Milburn. A classical channel model for gravitational decoherence. *New Journal of Physics*, 16(6):065020, jun 2014.
- [45] Antoine Tilloy and Lajos Diósi. Sourcing semiclassical gravity from spontaneously localized quantum matter. *Phys. Rev. D*, 93:024026, Jan 2016.
- [46] It is essential to remember that these gravitational interactions must be sourced by a quantum state.
- [47] Akira Matsumura. Path-entangling evolution and quantum gravitational interaction. *Phys. Rev. A*, 105:042425, Apr 2022.
- [48] Daisuke Miki, Akira Matsumura, and Kazuhiro Yamamoto. Feasible generation of gravity-induced entanglement by using optomechanical systems. *Phys. Rev. D*, 110:024057, Jul 2024.
- [49] Massimiliano Rossi, David Mason, Junxin Chen, and Albert Schliesser. Observing and verifying the quantum trajectory of a mechanical resonator. *Phys. Rev. Lett.*, 123:163601, Oct 2019.
- [50] Charles H. Bennett, David P. DiVincenzo, John A. Smolin, and William K. Wootters. Mixed-state entanglement and quantum error correction. *Phys. Rev. A*, 54:3824–3851, Nov 1996.
- [51] Robert B. Griffiths. Types of quantum information. *Phys. Rev. A*, 76:062320, Dec 2007.
- [52] A. Galindo and M. A. Martín-Delgado. Information and computation: Classical and quantum aspects. *Rev. Mod. Phys.*, 74:347–423, May 2002.
- [53] R. Simon. Peres-horodecki separability criterion for continuous variable systems. *Phys. Rev. Lett.*, 84:2726–2729, Mar 2000.
- [54] Lu-Ming Duan, G. Giedke, J. I. Cirac, and P. Zoller. Insseparability criterion for continuous variable systems. *Phys. Rev. Lett.*, 84:2722–2725, Mar 2000.
- [55] Ryszard Horodecki, Paweł Horodecki, Michał Horodecki, and Karol Horodecki. Quantum entanglement. *Rev. Mod. Phys.*,

- 81:865–942, Jun 2009.
- [56] A. C. Doherty and K. Jacobs. Feedback control of quantum systems using continuous state estimation. *Phys. Rev. A*, 60:2700–2711, Oct 1999.
- [57] Asa Hopkins, Kurt Jacobs, Salman Habib, and Keith Schwab. Feedback cooling of a nanomechanical resonator. *Phys. Rev. B*, 68:235328, Dec 2003.
- [58] Helge Müller-Ebhardt, Henning Rehbein, Chao Li, Yasushi Mino, Kentaro Somiya, Roman Schnabel, Karsten Danzmann, and Yanbei Chen. Quantum-state preparation and macroscopic entanglement in gravitational-wave detectors. *Phys. Rev. A*, 80:043802, Oct 2009.
- [59] Yakir Aharonov, Peter G. Bergmann, and Joel L. Lebowitz. Time symmetry in the quantum process of measurement. *Phys. Rev.*, 134:B1410–B1416, Jun 1964.
- [60] Farid Khalili, Stefan Danilishin, Haixing Miao, Helge Müller-Ebhardt, Huan Yang, and Yanbei Chen. Preparing a mechanical oscillator in non-gaussian quantum states. *Phys. Rev. Lett.*, 105:070403, Aug 2010.
- [61] Luc Bouten, Ramon Van Handel, and Matthew R. James. An introduction to quantum filtering. *SIAM Journal on Control and Optimization*, 46(6):2199–2241, 2007.
- [62] Norbert Wiener. *Extrapolation, interpolation, and smoothing of stationary time series: with engineering applications*. The MIT press, 1949.
- [63] P. Gibilisco and T. Isola. How to distinguish quantum covariances using uncertainty relations. *Journal of Mathematical Analysis and Applications*, 384(2):670–676, 2011.
- [64] A. I. Lvovsky and M. G. Raymer. Continuous-variable optical quantum-state tomography. *Rev. Mod. Phys.*, 81:299–332, Mar 2009.
- [65] Haixing Miao, Stefan Danilishin, Helge Müller-Ebhardt, Henning Rehbein, Kentaro Somiya, and Yanbei Chen. Probing macroscopic quantum states with a sub-heisenberg accuracy. *Phys. Rev. A*, 81:012114, Jan 2010.
- [66] H. J. Kimble, Yuri Levin, Andrey B. Matsko, Kip S. Thorne, and Sergey P. Vyatchanin. Conversion of conventional gravitational-wave interferometers into quantum nondemolition interferometers by modifying their input and/or output optics. *Phys. Rev. D*, 65:022002, Dec 2001.
- [67] Eric Chitambar, Debbie Leung, Laura Mančinska, Maris Ozols, and Andreas Winter. Everything you always wanted to know about locc (but were afraid to ask). *Communications in Mathematical Physics*, 328:303–326, 2014.
- [68] Heng Fan. Distinguishability and indistinguishability by local operations and classical communication. *Phys. Rev. Lett.*, 92:177905, Apr 2004.